Response to Reviewers' comments
Journal: Atmospheric Chemistry and Physics
Manuscript ID: EGUSPHERE-2025-1561
Title: "Measurement report: Impact of domestic heating on dust deposition sources in hyper-arid Qaidam Basin, northern Qinghai-Xizang Plateau"
Author(s): Haixia Zhu, Lufei Zhen, Suping Zhao*, Xiying Zhang*
*In the revised manuscript, revisions are marked in BLUE.

Editor's comments:
Reviewer #2:

The authors collected dust samples from six sites in the Qaidam Basin, over three years to investigate the impact of domestic heating on atmospheric dust in hyper-arid region. The OC/EC and char-EC/soot-EC ratios, along with PMF results, indicated that coal and biomass burning were the main contributors to dust deposition in rural, strongly influenced by domestic heating, whereas urban dust predominantly originated from vehicle and industrial emissions. This study provides a reference for investigating carbonaceous aerosols in climatically similar hyper-arid basins with intensive human activity and salt lake regions Overall, the results are well presented and discussed. It is publishable after the following questions have been well addressed.

1. The abstract of the current manuscript requires supplementation with more qualitative and quantitative descriptions, such as the significant differences in OC/EC ratios and the percentage contributions from PMF source apportionment. These additions would further highlight the key findings of this study.

Response:
Thank you for your insightful suggestions. The results section of the abstract has been revised accordingly to include additional qualitative and quantitative descriptions, as shown below.

Lines 37-47:
Among various carbon indicators, organic carbon (OC) and element carbon (EC) levels rose during the HP, with Char-EC as the primary component of EC (80.44%). Char-EC concentrations were higher in urban areas (85.00%), while secondary organic carbon (68.17%), the main contributor to OC, was more prevalent in rural (73.92%). The OC/EC ratio in urban areas remained stable with an average of 2.16. In contrast, the rural OC/EC ratio was significantly higher during the NHP (7.27 ± 4.66) than during the HP (4.57 ± 3.02). Additionally, the char/soot ratio was elevated in the HP (5.06 ± 4.08) compared to the NHP (4.42 ± 3.09). The OC/EC and char-EC/soot-EC ratios, along with PMF results, indicated that coal (17.28%) and biomass burning (32.50%) were the main contributors to dust deposition in rural, strongly influenced by domestic heating, whereas urban dust predominantly originated from traffic (44.43%) and industrial emissions (16.41%).

2. The manuscript should provide more detailed descriptions of the sampling sites, particularly regarding the sampler installation height and surrounding environment (e.g., distance from potential interference sources like roadways or chimneys). These specifications are crucial for evaluating potential sampling biases and ensuring reliability of the study. Does the collection efficiency of PM10/PM2.5 by the glass ball method need calibration?

Response:

We really appreciate your review and suggestions. This dust collector is a passive sampling device rather than an active size-segregated sampler; therefore, no calibration was performed. The design of our dust collector was primarily based on the Marble Dust Collector (MDCO) method (Ganor, 1975), which uses glass marbles to collect settling dust. According to Sow et al (2006), the collection efficiency of the MDCO decreases with increasing wind speed, dropping below 20% when wind speed exceeds 3 m/s, and it preferentially collects fine dust particles ranging from 10 to 31 μm in size (Chow, 1995). This type of collector has been widely used in numerous studies to evaluate local dust conditions (Abdollahi et al., 2021; Barjoee et al., 2021; Alzahrani et al., 2024). Therefore, we consider this collector effective for capturing fine dust particles, and the actual dust deposition flux can be estimated by accounting for its approximately 20% collection efficiency. In this study, dust samples were collected monthly, with each sampling period lasting 30 or 31 days. The collection bags were uniformly retrieved on the evening of the last day of each month and replaced with new ones. The relevant content has been added to the manuscript (**Lines 156-164**). The installation height and environment of the samplers are provided in Table S1.

Table S1 Geographic coordinates and descriptions of monitoring stations in the study area. The table lists the latitude and longitude of each site, along with a brief description of the local characteristics and land use. [XZH, Xiao Zaohuo station; GEM, Golmud station; LTC, Da Gele station; NMH, Nuo Muhong station; BLX, Balong station; DLX, Dulan station].

Stations	Latitude (°)	Longitude (°)	Description	Height (m)	Surrounding environment
XZH	93.68	36.80	*Lycium* berry cultivation base, national climate benchmark station	15	Sampler installed on the rooftop of a 3-story building at Xiaozhuohuo Meteorological Station. The area is open, with no other structures within 1 km; entirely agricultural land
GEM	94.91	36.42	The largest city in the Qaidam Basin, with a high population	10	Sampler placed on the rooftop of a 2-story building at Golmud Meteorological Bureau. Surroundings include public facilities; a road is 50 m away. Urban heating is primarily central or natural gas-based
LTC	95.77	36.49	Desert with camel breeding farms	3	Sampler located on the rooftop of a single-story building at Dageliao Camel Farm. The area is sparsely populated and largely undisturbed
NMH	96.43	36.44	Towns with extensive *Lycium* berry cultivation in the surrounding areas	1.5	Sampler installed at Nuomuhong Meteorological Station (~1.5 m above ground). Adjacent to a road. Local heating relies on household coal and biomass fuels
BLX	97.54	36.16	Pasture with developed agricultural practices	3	Sampler mounted on the rooftop of a single-story dwelling of a Tibetan herder in Balong Township. Sparse residential presence; distant from major roads
DLX	98.10	36.30	County seat with a relatively large population and a thriving mining industry	20	Sampler positioned on the rooftop of a 4-story building at Dulan Meteorological Bureau. Nearby roads present. Heating primarily from household coal and biomass fuels

3. The emission factors used in the PMF analysis (Section 3.6) require proper justification through established criteria or references to previous studies.

Response:

Thank you for your valuable suggestions and feedback. The source apportionment and factor identification for atmospheric PMF in this study were performed primarily in accordance with the standard *Ambient air, source apportionment on particulate matter, technical guide on positive matrix factorization model calculation* (HJ 1353-2024) issued by the Ministry of Ecology and Environment of the People's Republic of China. We acknowledge that the original manuscript did not sufficiently elaborate on the rationale for selecting characteristic elements for factor identification. In the revised manuscript, we have systematically clarified the representative marker species (e.g., SO_4^{2-}, NO_3^-, NH_4^+, and various metal elements) used for each factor and the basis for their selection in source identification. The specific additions are as follows:

Line 735:

Mg, Al, Si, and Fe are typical tracers for soil dust (Liu et al., 2003; Heo et al., 2009).

Lines 783-784:

Zhang et al (2023) found that coal combustion emits particles rich in Cl^-.

Line 751-759:

Elements and ions including V, NO_3^-, Ni, and carbonaceous components primarily associate with vehicle exhaust (Cong et al., 2011; Zhang et al., 2012). For instance, Ni can be emitted from fuel combustion and vehicle exhaust (Pacyna and Pacyna, 2001). In contrast, Cu, Zn, nps-Mg^{2+}, and nps-K^+ originate from non-exhaust vehicle emissions (brake and tire wear, and resuspended road dust) (Amato et al., 2014). For example, Zn may derive from rubber tire wear (Rogge et al., 1993), Pb emissions may be related to wear (tires/brakes) (Smichowski et al., 2007), and Cu is associated with brake wear (Lin et al., 2015).

Line 795:

K^+ serves as an important tracer for biomass burning (Cachier and Ducret, 1991).

Lines 811-814:

Zn, Cu, Fe, and Mn are also major chemical components in industrial emission profiles; Cd is a trace element found in metallurgical industries (Xu et al., 2022), while Zn and Mn emitte from oil combustion, metallurgy, and steel manufacturing processes (You et al., 2017). Pb and Cd are associated with metal smelting and processing (Fang et al., 2021).

Line 829:

High mass loadings of NO_3^- and SO_4^{2-} are characteristic of typical secondary inorganic aerosols (Huang et al., 2021).

4. The discussion would benefit from a systematic comparison of QDB's carbon composition

with data from other global regions.

Response:

We greatly appreciate your feedback. To further elucidate the significance of this study, we have supplemented the revised manuscript with a comparative analysis of carbonaceous components in atmospheric dust-fall from the Qaidam Basin (QDB) and data from various regions worldwide. It should be noted that due to fundamental differences in particle size and sampling method between atmospheric dust-fall and atmospheric particulate matter (e.g., PM_{10}, $PM_{2.5}$), and due to the fact that atmospheric dust-fall is a passively collected mixed sample whose sources and representativeness differ from actively collected samples like TSP, they were not directly compared in this study. Given the current limited systematic research on carbonaceous components in global atmospheric dust-fall, we introduced road dust carbonaceous element data from various environmental contexts as a reference to facilitate a meaningful comparison (Table S4). To ensure comparability, the selected road dust samples were directly collected as in-situ dust (without resuspension treatment).

We found that the concentrations of TC, OC, and EC in QDB (3.27, 1.88, and 1.41 mg/g, respectively) were significantly lower than those in industrial or urban areas such as Bolu, Turkey; New Delhi, India; and Ezhou, China, and were even lower than many other Chinese cities (Table S3). The low concentrations of OC and EC in QDB indicate minimal anthropogenic pollution influence in this region, and the data can represent the regional background values of carbonaceous components in atmospheric dust-fall in the arid inland areas of East Asia (Chen et al., 2019a). This is crucial for global models assessing the emission fluxes of carbonaceous aerosols from dust source regions. In contrast, extremely high values of carbonaceous elements were found primarily in urban road dust from locations like Bolu, Turkey (TC: 605.2 mg/g), Gwangju, South Korea (TC: 31.97 mg/g), and Xi'an, China (TC: 36.53 mg/g), indicating strong influences from traffic emissions (mainly non-exhaust emissions) (Wei et al., 2015; Lee et al., 2018; Demir et al., 2022). For atmospheric dust-fall in major cities like New Delhi, India, and Wuhan, China, the carbonaceous components are affected by the combination of traffic emissions (diesel vehicle emissions being a major source of EC), industrial activities, and emissions from dense populations (Deng et al., 2014; Zhang, 2014; Zhan et al., 2016; Mishra and Kulshrestha, 2017).

The OC/EC ratio in QDB (3.66) is at an intermediate level. It is much lower than that in regions dominated by biomass burning, such as Kumasi, West Africa (17.07) and Huainan, China (21.4), but is relatively close to ratios found in cities like Gwangju, South Korea (5.63) and Ulaanbaatar, Mongolia (5.69), albeit with significantly lower concentrations (Lee et al., 2018; Bandowe et al., 2019; Liu et al., 2020). We primarily analyzed the OC/EC ratios in cities across different regions of China to reveal the influence of economic development levels. The results show that the OC/EC values in atmospheric dust-fall are the lowest in Western China, intermediate in Central China, and the highest in Eastern China, mirroring the trend found for OC/EC in atmospheric particulate matter. This suggests that the carbonaceous elements in QDB dust-fall may primarily result from coal combustion and industrial emissions, leading to elevated EC concentrations and lower OC/EC ratios (Liu et al., 2022a). Conversely, economically developed cities with large populations and higher per capita incomes, such as Beijing and Tianjin, are influenced by secondary pollution, which typically leads to higher OC/EC ratios.

The Char/Soot ratio in QDB is notably high at 5.04, significantly exceeding that of other regions such as Xi'an (0.99) and Wuhan (0.09) (Wei et al., 2015; Liu et al., 2021). Char-EC primarily originates from incomplete combustion processes like biomass burning and coal combustion. Soot-EC mainly derives from high-temperature combustion sources such as fuel oil and diesel vehicle exhaust (Han et al., 2009). The exceptionally high Char/Soot ratio in QDB strongly indicates that its limited carbonaceous components predominantly originated from relatively inefficient combustion sources. These potentially included coal or small-scale biomass burning for local residential/expedition activities (e.g., heating, cooking) and possibly long-range transported biomass burning products (e.g., from forest/agricultural fires in South or Southeast Asia) (Han et al., 2009; Han et al., 2006; Han et al., 2016). In contrast, the very low Char/Soot ratios observed in cities like Wuhan and Xi'an clearly point to traffic source emissions as their primary contributor, a finding likely influenced by the specific focus of those studies on road dust.

However, we fully recognize the fundamental differences in sources and composition between road dust and atmospheric dust-fall. Road dust is primarily secondary dust formed from traffic activities, construction dust, soil particles, and resuspended deposited atmospheric particles, with its carbonaceous composition strongly reflecting intense local anthropogenic emissions (Casotti Rienda and Alves, 2021). In contrast, atmospheric dust-fall integrates contributions from local sources, regional transport, and even long-range transport. Therefore, direct comparison between these two may introduce bias when interpreting regional pollution characteristics and the degree of anthropogenic influence, which cannot be overlooked. Building on this analysis, the next phase of this research will focus on the sampling and analysis of fine atmospheric particulate matter (PM2.5 and PM1) to more accurately elucidate the emission levels and environmental and climatic impacts of carbonaceous aerosols in the Qaidam Basin. The relevant content has been added to the manuscript (**Lines 551-620**).

Table S4 Comparison of carbonaceous element concentrations in dust-fall from this study with those from other global regions.

Site	Souces	TC	OC	EC	OC/EC	Char-EC	Soot-EC	Char/soot	Reference
Gwangju (Korea)	Road dust	31.97	27.15	4.82	5.63	/	/	/	(Lee et al., 2018)
Ulaanbaatar (Mongolia)	Road dust	8.43	7.17	1.26	5.69	/	/	/	(Lee et al., 2018)
Bolu (Turkey)	Road dust	605.2	533	72.2	7.38	53.7	18.5	2.90	(Demir et al., 2022)
E'zhou (Hubei)	Road dust	18.29	5.35	12.84	0.42	/	/	/	(Zhang et al., 2016)
Kumasi (West African)	Road dust	28.00	26.45	1.55	17.07	1.19	0.36	3.31	(Bandowe et al., 2019)
Xian	Road dust	36.53	31.01	5.52	5.62	2.75	2.77	0.99	(Wei et al., 2015)

Huainan	Road dust	27.11	25.9	1.21	21.40	0.59	0.27	2.19	(Liu et al., 2020)
Guwahati (India)	Road dust	21.50	0.80	20.70	0.16	/	/	/	(Hussain et al., 2015)
Wuhan	Road dust	3.50	1.29	2.21	0.85	0.17	2.04	0.09	(Liu et al., 2021)
New Delhi (India)	Dust-fall	61.63	56.5	5.13	11.01	/	/	/	(Mishra and Kulshrestha, 2017)
Xian	Dust-fall	14.6	7.4	7.2	1.03	/	/	/	（Han et al., 2009）
Huangshi	Dust-fall	36.61	25.15	11.46	2.19	/	/	/	（Zhan et al., 2016）
Nanchang	Dust-fall	24.46	15.18	9.28	1.64	/	/	/	(Zhang, 2014)
Beijing	Dust-fall	47.2	41.5	5.7	8.9	/	/	/	(Tang et al., 2013)
Tianjin	Road dust	13.17	10.63	2.54	4.05	/	/	/	(Ma et al., 2019)
Shijiazhuang	Road dust	20.65	18.34	2.29	5.83	/	/	/	(Guo et al., 2018)
Wuhu	Dust-fall	33.26	22.49	10.77	2.09	/	/	/	(Deng et al., 2014)
Xiaogan	Dust-fall	5.77	4.32	1.45	2.98	/	/	/	(Zhan et al., 2022)
Qaidam Basin	Dust-fall	3.27	1.88	1.41	3.66	1.14	0.25	4.97	This study

5. The observed inverse trend in salt lake sources during HP periods necessitates more mechanistic explanation (line 550). Potential contributing factors might include: (1) wind speed or direction variations? (2) seasonal differences in salt lake activity? and (3) atmospheric transport differences caused by geographical location?

Response:

Thank you for your insightful suggestions. In our analysis of the salt lake source contribution, we found that it accounted for 5.48% during the heating periods (HP) and 20.32% during the non-heating periods (NHP) in rural areas, while in urban areas, it was 15.38% during the HP and 2.75% during the NHP, showing opposite trends. Backward trajectory simulations indicated that during the HP, air mass in both urban and rural areas mainly originated from the northwestern part of the basin and the eastern Tarim Basin, whereas during the NHP, they were broadly influenced by the salt lake within the basin (Figure S6). The minor wind direction differences and the inter-distributed sampling points suggests no substantial geographical disparity between urban and rural sites (Figure 1 in manuscript). Additionally, the ion content derived from playa salts in dust deposits increased during the NHP in both areas. Therefore, we propose that the anomalous increase in salt lake

contribution during the urban HP may be closely related to human activities.

The enhanced Urban Heat Island (UHI) effect and temperature inversion structures during the HP can alter boundary layer height, turbulence, and deposition conditions, thereby increasing the residence time of externally transported particles within the urban boundary layer and elevating their measured contribution (Cichowicz and Bochenek, 2024). Urban heat sources and heating emissions may also modify local transport pathways, leading to more concentrated deposition of dust originating from salt lake over urban areas. Furthermore, dry road surfaces, increased traffic, and construction activities during the HP can promote the resuspension of previously deposited playa dust. The use and subsequent resuspension of road de-icing salts (e.g., NaCl, $CaCl_2$) may further amplify the contribution of tracer ions indicative of playa salts (Gertler et al., 2006; Casotti Rienda and Alves, 2021). The relevant content has been added to the manuscript (**Lines 710-728**).

6. It is recommended to mark the percentage values in Figure 7 for clear comparison.

Response:

Thank you for your valuable suggestions and feedback. Percentages have been added to Figure 7b as recommended. However, the same modification could not be applied to Figure 7a due to the large number of species involved. Converting these values to percentages would compromise the clarity of the visual representation and obscure the key characteristic species for each factor.

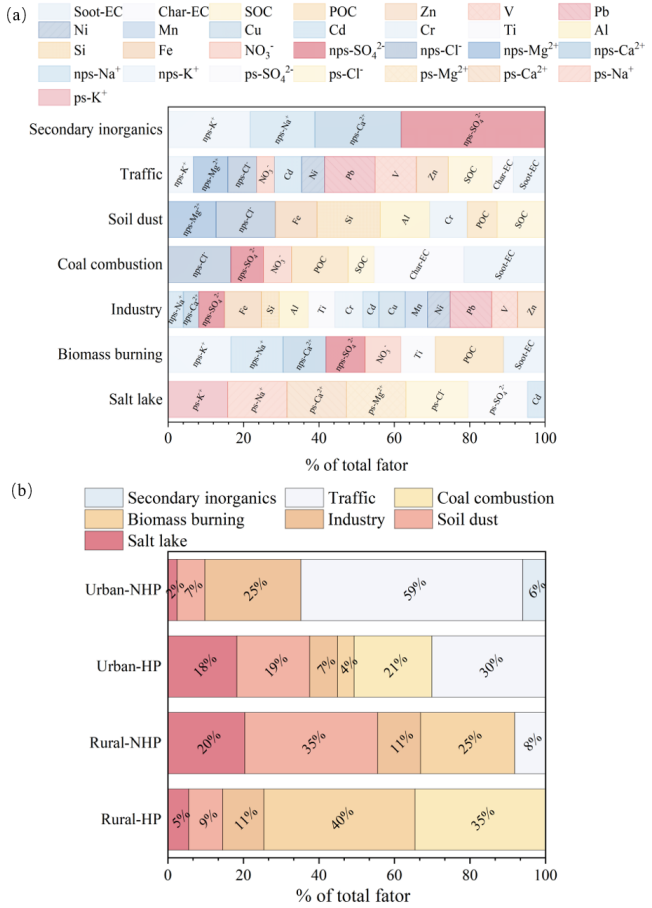

Figure 7 Factor profile and contributions in urban and rural areas. (a) presents the factor profiles, represented as the arithmetic mean of individual elements across various locations,

highlighting only those elements that constitute more than 20% of each profile. (b) illustrates the contributions of different sources at each location. [HP, domestic heating period; NHP, non-domestic heating period].

7. The authors should check through the whole manuscript very carefully for the revised version. Some mistakes should have been avoided if the authors carefully inspect the text before the submission. Such as line 33: "between2020" → "between 2020".

Response:

We sincerely thank the reviewer for this careful observation and for pointing out the typographical error. We apologize for this oversight. Furthermore, taking this comment seriously, we have conducted a thorough, line-by-line proofreading of the entire manuscript to identify and correct any similar formatting inconsistencies, spelling errors, or minor grammatical issues. We believe the language and formatting of the manuscript have now been significantly improved.

Reference

Abdollahi, S., Karimi, A., Madadi, M., Eslamian, S., Ostad-Ali-Askari, K., and Singh, V. P.: Lead concentration in dust fall in Zahedan, Sistan and Baluchistan Province, Iran, Journal of Geography and Cartography, 4, 6, 10.24294/jgc.v4i2.601, 2021.

Alzahrani, A. J., Alghamdi, A. G., and Ibrahim, H. M.: Assessment of soil loss due to wind erosion and dust deposition: Implications for sustainable management in arid regions, Applied Sciences, 14(23), 10822, 10.3390/app142310822, 2024.

Bandowe, B. A. M., Nkansah, M. A., Leimer, S., Fischer, D., Lammel, G., and Han, Y.: Chemical (C, N, S, black carbon, soot and char) and stable carbon isotope composition of street dusts from a major West African metropolis: Implications for source apportionment and exposure, Science of The Total Environment, 655, 1468-1478, https://doi.org/10.1016/j.scitotenv.2018.11.089, 2019.

Barjoee, S. S., Abadi, S. Z. M., Elmi, M. R., Varaoon, V. T., and Nikbakht, M.: Evaluation of trace elements pollution in deposited dust on residential areas and agricultural lands around Pb/Zn mineral areas using modified pollution indices, Journal of Environmental Health Science and Engineering, 19, 753-769, 10.1007/s40201-021-00643-8, 2021.

Casotti Rienda, I. and Alves, C. A.: Road dust resuspension: A review, Atmospheric Research, 261, 105740, https://doi.org/10.1016/j.atmosres.2021.105740, 2021.

Chen, P., Kang, S., Li, C., Zhang, Q., Guo, J., Tripathee, L., Zhang, Y., Li, G., Gul, C., Cong, Z., Wan, X., Niu, H., Panday, A. K., Rupakheti, M., and Ji, Z.: Carbonaceous aerosol characteristics on the Third Pole: A primary study based on the Atmospheric Pollution and Cryospheric Change (APCC) network, Environmental Pollution, 253, 49-60, https://doi.org/10.1016/j.envpol.2019.06.112, 2019.

Chow, J. C.: Measurement methods to determine compliance with ambient air quality standards for suspended particles, Journal of the Air & Waste Management Association, 45, 320-382, 10.1080/10473289.1995.10467369, 1995.

Cichowicz, R. and Bochenek, A. D.: Assessing the effects of urban heat islands and air pollution on human quality of life, Anthropocene, 46, 100433, https://doi.org/10.1016/j.ancene.2024.100433, 2024.

Demir, T., Karakaş, D., and Yenisoy-Karakaş, S.: Source identification of exhaust and non-exhaust traffic emissions through the elemental carbon fractions and Positive Matrix Factorization method,

Environmental Research, 204, 112399, https://doi.org/10.1016/j.envres.2021.112399, 2022.

Deng, Z., Fang, F., Jiang, P., Zhang, J., and Lin, Y.-S.: Distribution characteristics of black carbon in surface dust in Wuhu City, Journal of Anhui Normal University (Natural Science Edition), 37, 58-62, https://doi.org/10.14182/j.cnki.1001-2443.2014.01.009, 2014.

Gertler, A., Kuhns, H., Abu-Allaban, M., Damm, C., Gillies, J., Etyemezian, V., Clayton, R., and Proffitt, D.: A case study of the impact of Winter road sand/salt and street sweeping on road dust re-entrainment, Atmospheric Environment, 40, 5976-5985, https://doi.org/10.1016/j.atmosenv.2005.12.047, 2006.

Lee, K. Y., Batmunkh, T., Joo, H. S., and Park, K.: Comparison of the physical and chemical characteristics of fine road dust at different urban sites, Journal of the Air & Waste Management Association, 68, 812-823, 10.1080/10962247.2018.1443855, 2018.

Liu, P., Zhou, H., Chun, X., Wan, Z., Liu, T., Sun, B., Wang, J., and Zhang, W.: Characteristics of fine carbonaceous aerosols in Wuhai, a resource-based city in Northern China: Insights from energy efficiency and population density, Environmental Pollution, 292, 118368, https://doi.org/10.1016/j.envpol.2021.118368, 2022.

Liu, Y., Liu, G., Yousaf, B., Zhang, J., and Zhou, L.: Carbon fractionation and stable carbon isotopic fingerprint of road dusts near coal power plant with emphases on coal-related source apportionment, Ecotoxicology and Environmental Safety, 202, 110888, https://doi.org/10.1016/j.ecoenv.2020.110888, 2020.

Liu, Z., Cheng, J., Li, C., Gao, Y., Zhan, C.-L., Liu, S., Zhang, J., and Liu, H.: Pollution characteristics and source analysis of carbon components in road dust in Qingshan District, Wuhan City, Environmental Chemistry, 40, 772-778, 2021.

Mishra, M. and Kulshrestha, U.: Chemical characteristics and deposition fluxes of dust-carbon mixed coarse aerosols at three sites of Delhi, NCR, Journal of Atmospheric Chemistry, 74, 399-421, 10.1007/s10874-016-9349-1, 2017.

Wei, C., Bandowe, B. A. M., Han, Y., Cao, J., Zhan, C., and Wilcke, W.: Polycyclic aromatic hydrocarbons (PAHs) and their derivatives (alkyl-PAHs, oxygenated-PAHs, nitrated-PAHs and azaarenes) in urban road dusts from Xi'an, Central China, Chemosphere, 134, 512-520, https://doi.org/10.1016/j.chemosphere.2014.11.052, 2015.

Zhang, F.: Study on dry deposition of organic carbon and elemental carbon in the atmosphere of Nanchang City, [Master's thesis], 2014.

Reviewer #3：

This measurement report collects dust deposition samples from six urban and rural sites in the southern Qaidam Basin over the period from January 2020 to March 2023. It analyzes dust flux, water-soluble ions, trace elements, and carbonaceous components during domestic heating and non-heating periods, with the aims of identifying dust sources and assessing the impacts of heating activities. The report yields some interesting findings; however, it contains inconsistencies, and its PMF results require refinement—issues that may undermine the validity of its overall conclusions. First, OC and EC are typically the dominant components of aerosols from biomass or coal combustion (https://doi.org/10.3390/atmos13101595), yet the PMF source profiles presented here show higher trace metals and soluble ions instead. Second, aerosols from biomass or coal combustion are generally in the submicron size range (PM_1), which should correspond to lower mass compared to soil dust (primarily in the PM_{10} size mode, i.e., larger particles). This size-mass relationship is not adequately addressed, casting doubt on the accuracy of source contribution estimates. Third, the distinction between road dust and traffic-related emissions is blurred in the study, leading to an implausible conclusion. Vehicle-road interactions primarily drive the resuspension of road dust—a coarse-particle fraction—and brake emissions from vehicles are also a likely contributor. By contrast, traffic emissions from engine exhaust are dominated by submicron (PM_1) or ultrafine aerosols (https://acp.copernicus.org/articles/20/12721/2020/).

Additionally, the figures lack clear organization, hampering readability and the ability to cross-verify results with data. Given these critical issues, I recommend a major revision to address the concerns outlined above before the manuscript is suitable for publication.

Response:

We really appreciate your review and constructive suggestions. Please find below our point-by-point responses.

(1) This study focused solely on EC and OC as carbonaceous components, which were further speciated into soot-EC, char-EC, POC, and SOC PMF analysis revealed that coal and biomass combustion sources accounted for 83.94% of the total POC, 20.91% of SOC, 74.54% of char-EC, and 71.52% of soot-EC across all sampling sites. Compared to other identified sources, carbonaceous species contributed predominantly to the biomass and coal combustion factors. However, carbonaceous components alone was insufficient as primary tracers for specific sources such as biomass or coal combustion in the PMF apportionment process. It was necessary to incorporate other ions (e.g., nps-K^+, nps-Cl^-) and trace elements (e.g., Pb, Zn, Ni) as key marker species to distinguish sources like biomass burning, coal combustion, and traffic emissions (Simoneit, 2002; Sulong et al., 2019; Smichowski et al., 2007; Zhang et al., 2012; Lin et al., 2015). A limitation of this study is the lack of support from specific tracers such as levoglucosan in the source apportionment results. We will strengthen this aspect in future research. Moreover, the PMF receptor model is a statistical method that decomposes aerosol composition data into factors based on covariance. Compared to trace elements and water-soluble ions, the chemical profiles of carbonaceous species may exhibit overlapping characteristics or lack distinct source-specific signatures, making it a challenge for PMF to accurately separate and attribute their origins (Liu et

al., 2025).

(2) This study observed that the contribution of biomass burning to atmospheric dust deposition in rural areas of the Qaidam Basin during the heating period was higher than that of soil dust. Given that the collected dust samples had particle sizes >10 μm, while biomass burning typically emits aerosols in the submicron range, we propose several potential explanations. Firstly, during the HP, factors such as increased soil moisture and snow cover significantly suppress soil dust emission, resulting in a lower intensity than in other seasons (An et al., 2018; Yang et al., 2019). Simultaneously, biomass and coal burning for heating increases substantially, leading to intense, short-term emissions of fine particles. Although it was fine initially, these high-concentration ultrafine particles can undergo coagulation or coalescence, aggregating with each other or onto pre-existing coarse particles, thereby increasing their size (Butler and Mulholland, 2004; Kulmala et al., 2004; Li et al., 2020). Furthermore, fine particles from biomass burning (e.g., carbonaceous materials) may mix internally with coarse particles like soil dust or salt dust from the Qaidam Basin, forming internally mixed particles (Li et al., 2003; Hand et al., 2010). During source apportionment, such coarse particles are more likely to be attributed to the biomass burning source. Additionally, the Qaidam Basin is a significant source of salt dust (Zhu et al., 2025). Salt dust particles (e.g., halite, gypsum) provide excellent condensation nuclei for soluble substances emitted from biomass burning, greatly promoting hygroscopic growth (Li et al., 2003; Kumar, 2010; Wang, 2013). The basin's topography also favors stable inversion layers, inhibiting pollutant dispersion and allowing particles more time to grow, mix, and age in the atmosphere. Winter prevailing winds may also transport pollutants from surrounding regions into the basin. Finally, the PMF model may have uncertainties in resolving sources with similar chemical profiles. If the chemical compositions of local soil dust and biomass burning particles overlap after long-range transport and complex atmospheric reactions, the model might not fully separate them (Cesari et al., 2016). The relevant content has been added to the manuscript (**Lines 854-887**).

(3) We acknowledge that our previous analysis overlooked the contribution of road dust to traffic emissions. However, the particle size of the samples collected in this study is relatively large, while vehicle exhaust emissions are concentrated in submicron-sized aerosols. Therefore, the traffic emissions identified in this study should represent a mixture of vehicle exhaust (tailpipe emissions) and non-exhaust sources (e.g., tire and brake wear, and resuspended road dust). Characteristic elements for this source include V, NO_3^-, Ni, Cu, Zn, nps-Mg^{2+}, nps-K^+, and carbonaceous components. Specifically, Zn originates from the wear of rubber tires on roads (Rogge et al., 1993), Pb emissions are associated with wear (tires/brakes) (Smichowski et al., 2007), and Cu is linked to brake wear (Lin et al., 2015). Furthermore, the presence of crustal elements and ions such as Fe, Si, and nps-Mg^{2+} in the traffic emission factor for Urban-NHP, Urban-HP, and Rural-NHP likely derives from resuspended road dust (Chen et al., 2019). Consequently, a discussion regarding vehicle non-exhaust emissions has been added to the manuscript (**Lines 751-761**).

Line 145. Please provide more details about the dust collection techniques, including the dust size cut. Are you measuring total atmospheric dust with no size cut? Specify the dust collection efficiency, and the duration of each collection—for example, is it 24 hours?

Response:

We greatly appreciate your feedback. The dust collection in this study did not involve precise size-segregated sampling; instead, the collector utilized glass marbles to prevent resuspension of deposited dust and minimize contamination from large impurities. To effectively quantify atmospheric deposition, surrogate surfaces or deposition traps are commonly employed in field measurements. Surrogate surfaces are designed to replicate natural surfaces, offering easy deployment, compatibility with the surrounding environment, and minimal disturbance to airflow. Examples include glass marbles (Ganor, 1975; Offer et al.,1992; Offer et al., 1992), moist filter paper (Goossens and Offer, 1993), plastic surfaces (Gregory, 1961), and water or antifreeze-filled containers (Smith and Twiss, 1965). Our dust collector was primarily designed based on the Marble Dust Collector (MDCO) (Ganor, 1975), which uses glass marbles to collect settling dust. According to Sow et al (2006), the collection efficiency of the MDCO decreases with increasing wind speed, dropping below 20% when wind speed exceeds 3 m/s, and it preferentially collects finer dust particles (10–31 μm) (Chow, 1995). This type of collector has been widely used in many studies to assess local dust deposition (Abdollahi et al., 2021; Barjoee et al., 2021; Alzahrani et al., 2024). Therefore, we consider this collector effective for capturing fine dust particles, and the actual dust deposition flux can be estimated by accounting for the 20% collection efficiency. In this study, dust samples were collected monthly, with a sampling duration of 30 or 31 days. Collection bags were uniformly retrieved on the evening of the last day of each month and replaced with new ones. The relevant content has been added to the manuscript (**Lines 156-164**).

Line 204. Is OC fully collected on the filter samples? It is unclear whether the filter samples can collect all OC in the dust samples.

Response:

Thank you for your insightful suggestions. The method used in this study was established by Han et al (2007) to remove interference from minerals and silicates in soil, sediment, and atmospheric dust for the determination of carbonaceous components. It has been widely applied in measuring OC and EC in lake sediments and urban soils (Han et al., 2009; Khan et al., 2009; Han et al., 2011). This method shows an EC collection efficiency of approximately 99.6% (Zhan et al., 2013); however, no study has yet evaluated the OC collection efficiency. Han et al (2007) reported that the variation for OC after acid treatment ranged from 4.5% to 13.4%, mainly due to washing losses from colloid suspension formation and uneven residue distribution on filters. Analysis of five pre-treated blank samples showed similar OC levels to pre-combusted quartz filter blanks, indicating that acid pretreatment does not affect carbon determination (Han et al., 2007). In our study, the acid-treated supernatant was filtered onto pre-combusted quartz fiber filters. While quartz fiber filters retain >99.99% of particles larger than 0.3 μm, the retention efficiency for liquid suspensions remains unclear (Torres et al., 2014). Relevant content has been added to the manuscript (**Lines 218-221**).

This method has been widely applied to measure OC and EC contents in lake sediments and urban soils (Han et al., 2009; Khan et al., 2009; Han et al., 2011). Studies have shown that the EC collection efficiency of this method is approximately 99.6% (Zhan et al., 2013); however, its OC collection efficiency remains unclear.

Line 231. For biomass burning, OC/EC can exceed 2 even for primary emissions.

Response:
We agree with the reviewer that this sentence was inappropriate and have deleted it from the manuscript.

Line 247. Provide more details about the minimum R^2. Were all data analyzed together, or separately for the 6 sites? What is the specific minimum R^2 value for the data? Given the low time resolution of the method, I suspect OC and EC are well correlated, so the minimum R^2 method may not be suitable for this type of data.

Response:
Thank you for your valuable suggestions and feedback. We employed the Minimum R-squared (MRS) method (Millet et al., 2005; Wu and Yu, 2016; Wu et al., 2018a) to calculate the (OC/EC)pri ratio, which was subsequently used to derive SOC and POC concentrations. The computational procedure followed the algorithm developed by Wu and Yu (2016) (available at: https://sites.google.com/site/wuchengust), implemented within the Igor Pro environment (WaveMetrics, Inc., Lake Oswego, OR, USA). Due to the limited dataset size and low temporal resolution, the MRS analysis was performed collectively across all sampling sites. In this approach, the coefficient of determination (R^2) between SOC and EC was calculated iteratively for a range of $(OC/EC)_{pri}$ values of 0 to 10. The minimum R^2 value of 1.33 (Figure S2) identified the optimal $(OC/EC)_{pri}$ representative of the true primary ratio. Relevant content has been added to the manuscript (**Lines 268-274**).

The MRS method identifies the $(OC/EC)_{pri}$ value that minimizes the correlation between SOC and EC. Regression analyses of OC and EC across all Qaidam Basin sites, including urban/rural and heating/non-heating period subsets, consistently yielded weak correlations ($R^2 < 0.4$) (Figure 1). This low correlation validates the applicability of the MRS method for this dataset (Liu et al., 2023).

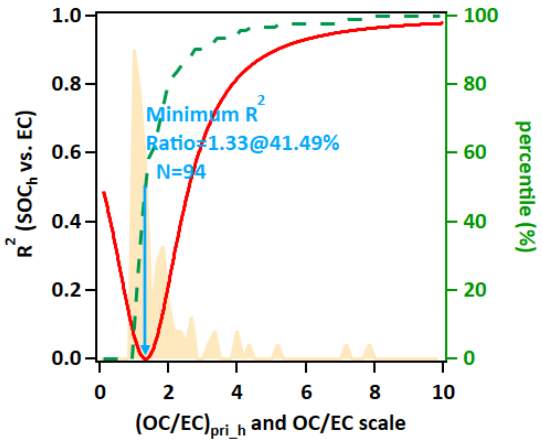

Figure S2 (OC/EC) ratio when minimum R^2 is observed between SOC and EC measurement data. The $(OC/EC)_{pri\_h}$ is defined as the hypothetical primary OC/EC ratio. The red line plots the R^2 between the tracer species (EC) for each value of $(OC/EC)_{pri\_h}$ (X-axis) and the estimated secondary organic carbon (SOC_h). The shaded area is the frequency distribution of the OC/EC ratio,

and green percentile represents the cumulative frequency rate. N represents the number of the total measurement data set.

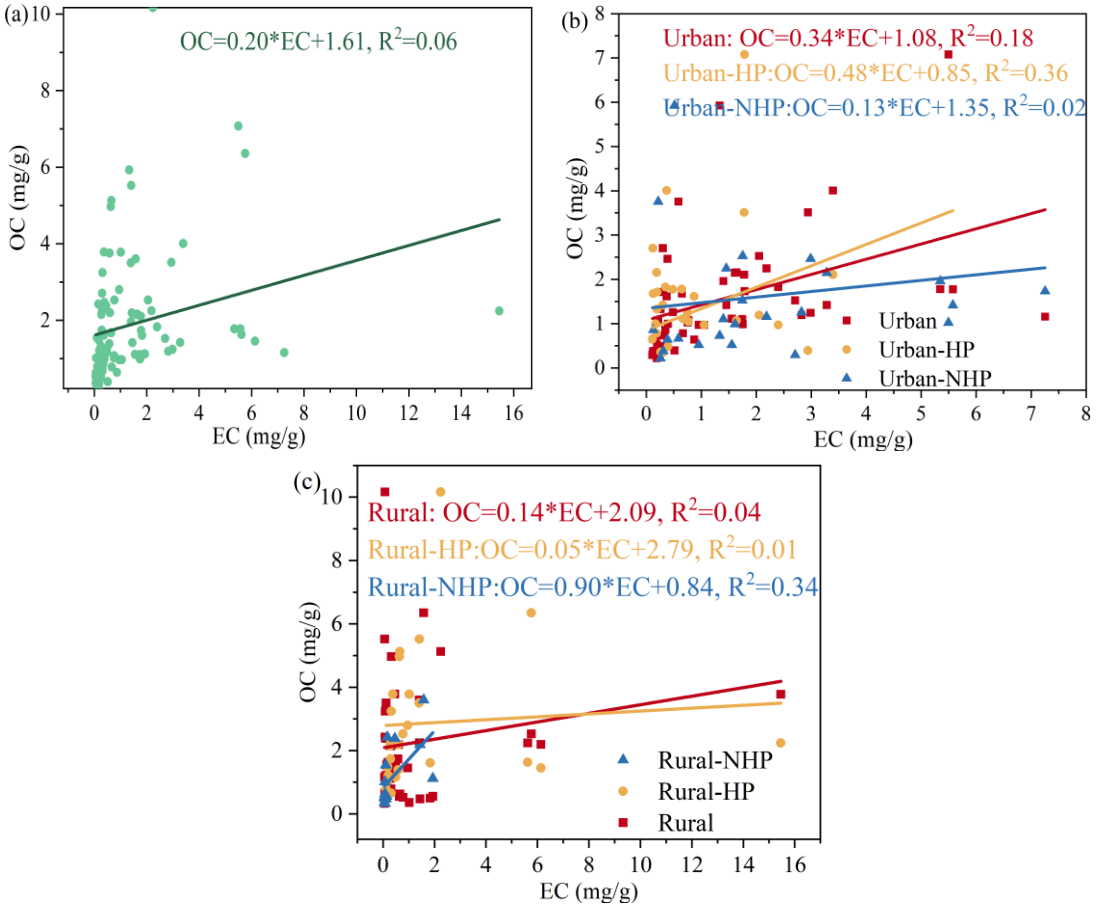

Figure 1. Correlation between OC and EC at: (a) all sampling sites, (b) urban and (c) rural sites during HP and NHP in the Qaidam Basin. HP, domestic heating period; NHP, non-domestic heating period.

In the Supporting Text, should Figure S14 be Figure S13?

Response:

We sincerely apologize for any confusion caused by our oversight. We thank the reviewer for pointing it out, and it has been corrected in the Supplementary file.

Line 295. How many runs were conducted for BS? What are the uncertainties of the PMF analysis? This should be evaluated, considering the small number of data points for each PMF run.

Response:

The BS analysis was run 20 times as required by the PMF User Guide. In this study, the decrease in DISP %dQ remained within 0.1%, indicating that the global minimum of dQ was achieved under these settings. No factor swaps occurred during the DISP analysis across four dQmax levels, and the BS factor matching rate exceeded 85%. Furthermore, no factor swaps were observed during the BS-DISP analysis, confirming the stability of the PMF model results (Paatero et al., 2014; Brown

et al., 2015; Li, 2020). Additionally, the results from the uncertainty tools provided in PMF 5.0 were analyzed (Table S3). Among these sources, the salt lake and secondary inorganic aerosol factors exhibited high uncertainty, influenced by the resampling of peak events rather than low (or zero) values. In contrast, the results for biomass/coal combustion and industrial emissions were highly stable, as indicated by the three rotational tools. The higher uncertainty in the BS and BS-DISP results suggests that many peak events affect these factors, which may not be adequately resampled in the BS runs, leading to greater uncertainty.

Beyond the uncertainty analysis, we evaluated the accuracy of the PMF source apportionment by analyzing the error in the temporal contribution of each source. The results presented in Table S6 are based on the dust deposition flux of each source (Manousakas et al., 2017). The following explanation has been added to Section 3.6 (**Lines 691-699**):

The uncertainty of the source contributions was calculated directly from the standard error of the multiple regression coefficients between the deposition flux (independent variable) and the source contribution (dependent variable) at different monitoring sites (Belis et al., 2015; Manousakas et al., 2017). The regression method assumes that all factors explaining the mass have been identified; however, if a significant portion of the mass not directly related to the species in the PMF analysis is omitted, the source contributions may be overestimated, which could be an important additional source of uncertainty. The results are shown in Table S6. It must be noted that this method captures only a portion of the total uncertainty, as it does not include errors from profile uncertainty or rotational ambiguity. The low errors calculated by this method indicate a good model fit.

Table S3 Uncertainty tools' results for dust deposition flux (mg/g).

	Base Value	BS 5th	BS 50th	BS 95th	DISP Min	DISP Average	DISP Max	BS-DISP 5th	BS-DISP average	BS-DISP 95th
Salt lake	1.2	0.2	1.8	3.5	0.1	1.5	1.6	0.0	3.2	4.9
Biomass burning	1.8	1.5	2.0	3.7	1.6	1.8	2.0	1.0	2.2	4.6
Industry	1.7	0.4	1.8	3.3	0.6	1.7	1.8	0.1	2.5	3.7
Coal combustion	1.8	0.1	1.6	2.1	0.5	1.8	2.1	0.0	1.4	3.8
Soil dust	1.4	0.6	1.3	2.0	0.3	1.2	1.6	0.4	0.9	3.8
Traffic emission	2.2	0.1	1.7	3.3	1.0	2.1	2.2	0.0	1.6	5.2
Secondary formation	1.2	0.0	1.3	2.2	0.2	1.2	1.2	0.0	2.1	4.2

Table S6 Sources contribution and corresponding error. HP, heating period; NHP, non-heating period.

	Rural-HP		Rural-NHP		Urban-HP		Urban-NHP	
	Contribution	Error	Contribution	Error	Contribution	Error	Contribution	Error

Industry	10.86	0.24	11.33	0.32	7.37	0.28	25.44	0.44
Salt lake	5.49	0.49	20.37	0.47	18.25	0.59	2.42	1.11
Soil dust	9.04	0.50	35.19	0.40	19.30	0.20	7.36	0.47
Coal combustion	34.57	0.30	N/A	N/A	20.63	0.37	N/A	N/A
Traffic emission	N/A	N/A	8.17	0.47	30.07	0.21	58.79	0.28
Biomass burning	40.05	0.28	24.95	0.71	4.38	0.35	N/A	N/A
Secondary inorganics	N/A	N/A	N/A	N/A	N/A	N/A	6.00	0.90

Why perform PMF separately for heating/non-heating periods and urban/non-urban areas? The factors appear similar except for coal combustion. Can all data be combined for a single PMF analysis? What type of industry does the expected industry factor correspond to?

Response:

We really appreciate your review and suggestions. Our study focuses on the impact of residential heating on atmospheric dust deposition in the QDB. Consequently, the PMF analysis was conducted separately for the HP and NHP. Based on the surrounding environment of the dust monitoring sites, sampling locations were categorized into urban and rural areas. These two types of locations utilize different fuels for heating: urban areas primarily use coal, natural gas, or electricity, whereas rural areas rely more on coal and biomass fuels. Therefore, separate PMF source apportionment was performed for urban and rural dust samples.

We believe that conducting separate PMF analyses maximizes the capture of unique, subtle pollution sources specific to each region and season, and more accurately reflects the variations in source profiles across seasons and regions. While integrating all data would increase sample size and potentially enhance model robustness, the results might lack the resolution needed to accurately characterize certain local sources (Srivastava et al., 2021). Thus, we consider that separate analyses for different regions and seasons are more appropriate for highlighting the impact of residential heating, and are well-suited to the objectives of this study.

Our analysis revealed distinct differences in dust sources across regions and seasons. For instance, no traffic emission source was identified in Rural-HP, while no coal combustion source was found in Rural-NHP. Conversely, Urban-NHP showed no coal or biomass burning sources but included a secondary inorganic aerosol source. These differences further justify the separate analysis approach. The QDB is rich in non-ferrous metal resources such as lead-zinc ores, oil, natural gas, and saline minerals (e.g., potassium, lithium). Consequently, the primary industrial activities in this region are mining and associated chemical industries. We identified industrial emissions using characteristic elements in the dust, including Pb (55.18%), Fe (48.91%), Cr (37.05%), Zn (36.42%), Ti (35.10%), Cu (34.91%), V (34.44%), Ni (29.69%), Mn (29.59%), and Cd (21.29%). The following content has been added to the manuscript (**Lines 820-826**):

Due to the abundance of non-ferrous metal resources (e.g., lead-zinc ores), oil, natural gas, and saline minerals (e.g., potassium, lithium) in the QDB, the primary industrial activities are mining and associated chemical industries. Particularly around the GEM and DLX sites, the presence of numerous lead-zinc, iron, and copper mining enterprises leads to significant contributions from

industrial emissions to urban dust fallout, making it one of the major sources of air pollution in the basin.

PMF analysis conducted on the pooled dataset (all periods and sites combined) for the Qaidam Basin identified six primary sources of atmospheric dust deposition (Figure 2): Coal Combustion (14.77%): Characterized by nps-Cl^- (58.89%), nps-Mg^{2+} (44.30%), nps-SO_4^{2-} (35.46%), SOC (40.07%), Char-EC (35.99%), POC (33.46%), and Soot-EC (28.00%) (Johnson et al ., 2006; Kundu et al, 2010); Traffic Emissions (24.39%): Dominated by Cd (67.36%), Zn (60.79%), Pb (60.33%), nps-Cl^- (36.57%), Cu (50.38%), Cr (44.89%), Ni (43.98%), Mn (43.51%), NO_3^- (35.30%), Char-EC (45.18%), SOC (30.29%), and Soot-EC (26.73%) (Adeniran et al., 2017). The presence of nps-Mg^{2+} (44.13%), nps-Cl^- (35.57%), and Si (26.73%) also indicates a contribution from road dust (non-exhaust emissions, e.g., wear and resuspension). Salt Lake Emissions (8.76%): Identified by ps-Na^+ (85.92%), ps-Ca^{2+} (85.93%), ps-SO_4^{2-} (85.93%), ps-Mg^{2+} (85.81%), ps-Cl^- (84.51%), and ps-K^+ (84.46%) (Ambade et al., 2022; Aswini et al., 2022; Gluscic et al., 2023; Wu et al., 2024). Industrial Emissions (13.82%): Marked by Ti (92.05%), Fe (88.29%), V (72.96%), Cr (41.98%), Pb (39.67%), Mn (36.31%), Zn (35.57%), Cu (30.94%), Si (27.25%), and Ni (22.96%) (Almeida et al., 2015; Yao et al., 2016). Biomass Burning (18.48%): Characterized by nps-K^+ (44.18%), NO_3^- (40.10%), nps-Na^+ (20.63%), Soot-EC (24.42%), and POC (32.88%) (Simoneit, 2002; Sulong et al., 2019). Soil Dust (19.77%): Identified by Al (80.80%), nps-Na^+ (79.37%), nps-SO_4^{2-} (62.99%), nps-Ca^{2+} (60.59%), and Si (27.30%) (Pervez et al., 2018; Tian et al., 2021).

The source profiles from this pooled analysis are generally consistent with those identified in our separate analyses. However, the time-series data from the pooled model failed to reveal the distinct source characteristics specific to different sampling sites and seasons (Figure 3). Therefore, we argue that conducting separate PMF analyses is more appropriate for capturing these spatiotemporal variations. Furthermore, our prior error analysis confirmed that, despite the smaller sample sizes in the separate analyses, the PMF results remain within an acceptable uncertainty range, supporting their reliability.

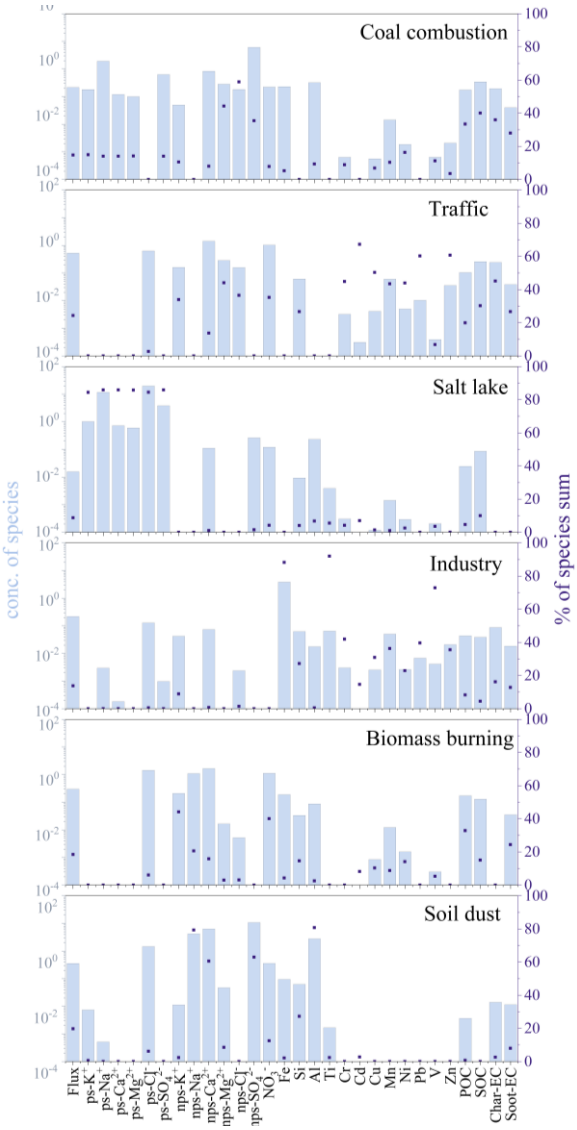

Figure 2 PMF source appointment of atmospheric dust deposition in the Qaidam Basin.

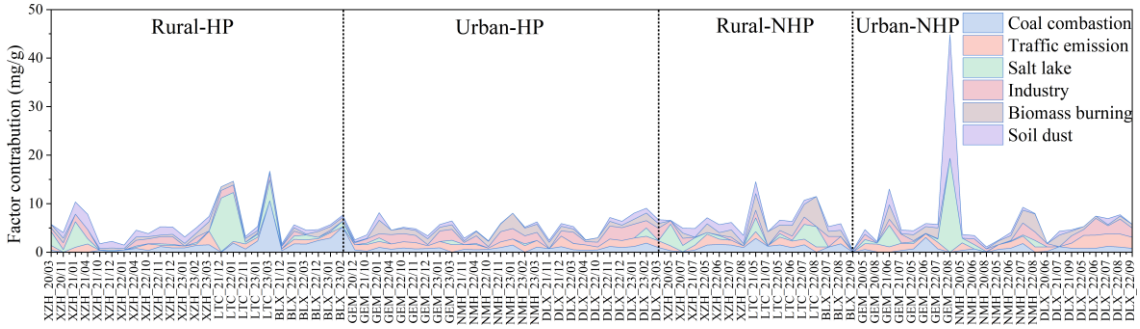

Figure 3 Temporal variations in factor contributions to atmospheric dust deposition in the Qaidam Basin. HP, domestic heating period; NHP, non-domestic heating period.

Line 309. Can the hypothesis be supported by the PMF results?

Response:

We propose that the increase in traffic emissions during the NHP may be linked to tourism activity.

Analysis of the PMF source apportionment time series revealed that traffic emission contributions in both rural and urban areas peaked during the 2022 NHP, specifically concentrated in July, August, and September, which coincides with the tourism high season. Due to the impact of the COVID-19 pandemic, tourist numbers in the Qaidam Basin sharply declined in 2020 and 2021. The peak in tourism activity in 2022 (Qinghai Statistical Yearbook, 2022) corresponded with the highest level of traffic emissions during the three-year period, indicating a direct impact of tourism flux on emission levels. However, given the relatively short sampling duration of this study (three years), longer-term data and further research are needed to substantiate this hypothesis. The relevant section in the manuscript has been revised (**Lines 761-769**).

Line 335. Are you suggesting that urban residents use more coal than rural residents? I would expect rural residents to use more coal, while urban areas have municipal central heating. This seems consistent with Line 377, which states rural carbon emissions are higher than urban levels.

Response:

Thank you for your insightful suggestions. The nps-SO_4^{2-}/NO_3^- ratio in soluble ions directly reflects the relative importance of sulfuric and nitric acids in the atmosphere, the precursors of which (SO_2 and NO_x) typically originate from different pollution sources. A high ratio (typically > 3) suggests dominance by stationary sources, such as coal-fired power plants and industrial boilers, where SO_2 emissions are the primary source of sulfate. A low ratio (typically < 1) indicates dominance by mobile sources, i.e., vehicle emissions where NO_x are the main contributors to nitrate (Pipal et al., 2019). It is important to note that "stationary sources" should not be interpreted solely as coal combustion but also include industrial emissions and long-range transport of sulfate from upwind industrial areas. The high ratio does not necessarily imply greater coal usage but rather indicates that industrial emissions, along with coal and biomass combustion, contribute more significantly to the soluble ion composition in urban dust-fall. Furthermore, due to the Urban Heat Island effects, the chemical reactions involving soluble ions in urban and rural atmospheres may differ under varying meteorological conditions like temperature and relative humidity, leading to changes in nps-SO_4^{2-} and NO_3^- concentrations (Putaud et al., 2003; Qiu et al., 2023). Therefore, conclusions cannot be drawn based solely on the nps-SO_4^{2-}/NO_3^- ratio; further analysis incorporating atmospheric emission inventories, source tracers, aerosol physicochemical processes, and meteorological conditions is essential. The original description was unclear and has been revised as follows (**Lines 363-372**):

The higher nps-SO_4^{2-}/NO_3^- ratio in urban areas compared to rural areas (Figure S7) indicates that during the study period, stationary sources (e.g., industrial emissions, coal, and biomass combustion) contributed more significantly to the ionic composition of urban dust fallout (Pipal et al., 2019). In contrast, the ratio was considerably lower during the NHP than during HP, suggesting that mobile sources likely played a more important role in the dust ionic composition during the NHP. Generally, emissions from coal combustion and biomass burning was intensified in northern China during the HP (Liu et al., 2016), while vehicle emissions dominate during the NHP (Xu et al., 2012), supporting the reliability of this analysis. Nevertheless, further investigation integrating atmospheric emission inventories, source tracers, aerosol physicochemical processes, and meteorological conditions is

warranted.

Line 398. The lower OC/EC ratios may be due to the low OC collection efficiency of the method used.

Response:

We greatly appreciate your feedback. The potential influence of OC collection efficiency during the pretreatment process, as rightly pointed out, represents a key limitation of this study and may introduce uncertainty into the interpretation of the OC/EC ratios. Accordingly, we have added the following statement in **Lines 587-590** of the revised manuscript to alert readers to this potential bias:

Lines 587-590:

Furthermore, as the pretreatment used in this study removes impurities such as silicates from the carbonaceous components of dust, and the OC collection efficiency of this treatment is currently unknown, the lower OC/EC ratios observed may also be attributed to a lower OC collection efficiency.

Line 419. I don't think comparing dust deposition (presumably TSP) with PM2.5, PM10, or filter samples is meaningful. Particles of different sizes have different sources, so you should compare with dust deposition data from literature, not filter samples.

Response

We appreciate the insightful comment. In this section, we originally compared the OC/EC ratios in dust deposition across different elevations in the Qaidam Basin with those reported for TSP, $PM_{2.5}$, and PM_{10} from various locations on the Qinghai-Xizang Plateau, aiming to elucidate the influence of altitude on carbonaceous components. However, significant differences in particle size distributions and sources between $PM_{2.5}$/PM_{10} and dust deposition samples were noted. Although our analyzed deposition samples (as shown in Figure S16) exhibited a particle size distribution with 89.70% of particles below 100 μm, which is somewhat comparable to TSP, a direct comparison remains inappropriate. This is primarily due to fundamental methodological differences: our study employed passive sampling over an extended period, whereas TSP data are typically derived from active filter sampling over 24–48 h. These differences in collection methods and sampling durations introduce substantial biases that preclude a meaningful comparison. Therefore, this section has been removed from the manuscript. Instead, we analyzed the characteristics of carbonaceous components in the Qaidam Basin dust by benchmarking their contents against those reported in atmospheric dust-fall and non-resuspended road dust from various global regions. The detailed data has now been provided in Table S4 and discussed in the manuscript (**Lines 551-620**).

Lines 551-620:

This study conducted a comparative analysis of carbonaceous element concentrations in atmospheric dust-fall and road dust between the QDB and other global regions (Table S4). To ensure data comparability, the selected road dust samples consisted of directly collected in-situ dust without resuspension treatment. The results revealed that the concentrations of TC, OC, and EC in QDB (3.27, 1.88, and 1.41 mg/g, respectively) were significantly lower than those in industrial or urban

areas such as Bolu, Turkey; New Delhi, India; and Ezhou, China, and were even lower than many other Chinese cities (Table S4). The low concentrations of OC and EC in QDB indicate minimal anthropogenic pollution influence in this region, and the data can represent the regional background values of carbonaceous components in atmospheric dust-fall in the arid inland areas of East Asia (Chen et al., 2019a). This is crucial for global models assessing the emission fluxes of carbonaceous aerosols from dust source regions. In contrast, extremely high values of carbonaceous elements were found primarily in urban road dust from locations like Bolu, Turkey (TC: 605.2 mg/g), Gwangju, South Korea (TC: 31.97 mg/g), and Xi'an, China (TC: 36.53 mg/g), indicating strong influences from traffic emissions (mainly non-exhaust emissions) (Wei et al., 2015; Lee et al., 2018; Demir et al., 2022). For atmospheric dust-fall in major cities like New Delhi, India, and Wuhan, China, the carbonaceous components are affected by the combination of traffic emissions (diesel vehicle emissions being a major source of EC), industrial activities, and emissions from dense populations (Deng et al., 2014; Zhang, 2014; Zhan et al., 2016; Mishra and Kulshrestha, 2017).

The OC/EC ratio in QDB (3.66) is at an intermediate level. It is much lower than that in regions dominated by biomass burning, such as Kumasi, West Africa (17.07) and Huainan, China (21.4), but is relatively close to ratios found in cities like Gwangju, South Korea (5.63) and Ulaanbaatar, Mongolia (5.69), albeit with significantly lower concentrations (Lee et al., 2018; Bandowe et al., 2019) (Liu et al., 2020). We primarily analyzed the OC/EC ratios in cities across different regions of China to reveal the influence of varying economic development levels.

Figure 5a presents spatial variations in urban OC/EC ratios across China. The findings reveal that the Northwest region, represented by QDB urban and Xi'an (XA) (Han et al., 2009b), exhibits a significantly lower ratio (1.59 ± 0.56) compared to central regions, including Nanchang (NC) (Zhang, 2014), Huangshi (HS) (Zhan et al., 2016), Wuhu (WH) (Deng et al. 2014), Xiaogan (XG) (Zhan et al., 2022), and Huainan (HN) (Liu et al., 2020), where the ratio is 5.86 ± 7.81. This ratio is also lower than that observed in eastern cities such as Beijing (BJ) (Tang et al., 2013), Tianjin (TJ) (Ma et al., 2019), and Shijiazhuang (SJZ) (Guo et al., 2018), which have a ratio of 6.83 ± 2.77. This pattern is consistent with the trends in atmospheric PM OC/EC ratios (Xie et al., 2023), suggesting that the carbon in the dust of the QDB urban primarily results from coal combustion and industrial emissions, leading to elevated EC concentrations and lower OC/EC ratios (Liu et al., 2022). Conversely, cities with higher economic development, such as Beijing and Tianjin, characterized by greater population density and income levels, typically experience secondary pollution, resulting in higher OC/EC ratios. Furthermore, as the pretreatment used in this study removes impurities such as silicates from the carbonaceous components of dust, and the OC collection efficiency of this treatment is currently unknown, the lower OC/EC ratios observed may also be attributed to a lower OC collection efficiency.

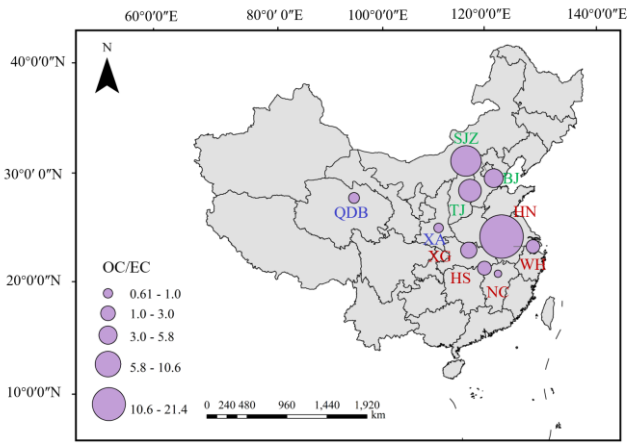

Figure 5 Distribution of OC/EC ratios across various regions of China. Blue designations represent the Northwest region, red indicates the Central region, and green denotes the Eastern region. The circle size reflects the magnitude of the OC/EC ratios.

The Char/Soot ratio in QDB is notably high at 5.04, significantly exceeding that of other regions such as Xi'an (0.99) and Wuhan (0.09) (Wei et al., 2015; Liu et al., 2021). Char-EC primarily originates from incomplete combustion processes like biomass burning and coal combustion. Soot-EC mainly derives from high-temperature combustion sources such as fuel oil and diesel vehicle exhaust (Han et al., 2009). The exceptionally high Char/Soot ratio in QDB strongly indicates that its limited carbonaceous components predominantly originated from relatively inefficient combustion sources. These potentially included coal or small-scale biomass burning for local residential/expedition activities (e.g., heating, cooking) and possibly long-range transported biomass burning products (e.g., from forest/agricultural fires in South or Southeast Asia) (Han et al., 2009; Han et al., 2006; Han et al., 2016). In contrast, the very low Char/Soot ratios observed in cities like Wuhan and Xi'an clearly point to traffic source emissions as their primary contributor, a finding likely influenced by the specific focus of those studies on road dust.

However, we fully recognize the fundamental differences in sources and composition between road dust and atmospheric dust-fall. Road dust is primarily secondary dust formed from traffic activities, construction dust, soil particles, and resuspended deposited atmospheric particles, with its carbonaceous composition strongly reflecting intense local anthropogenic emissions (Casotti Rienda and Alves, 2021). In contrast, atmospheric dust-fall integrates contributions from local sources, regional transport, and even long-range transport. Therefore, direct comparison between these two may introduce bias when interpreting regional pollution characteristics and the degree of anthropogenic influence, which cannot be overlooked. Building on this analysis, the next phase of this research will focus on the sampling and analysis of fine atmospheric particulate matter (PM2.5 and PM1) to more accurately elucidate the emission levels and environmental and climatic impacts of carbonaceous aerosols in the QDB.

Table S4 Comparison of carbonaceous element concentrations in dust-fall from this study with those from other global regions.

Site	Souces	TC	OC	EC	OC/EC	Char-EC	Soot-EC	Char/soot	Reference
Gwangju (Korea)	Road dust	31.97	27.15	4.82	5.63	/	/	/	(Lee et al., 2018)
Ulaanbaatar (Mongolia)	Road dust	8.43	7.17	1.26	5.69	/	/	/	(Lee et al., 2018)
Bolu (Turkey)	Road dust	605.2	533	72.2	7.38	53.7	18.5	2.90	(Demir et al., 2022)
E'zhou (Hubei)	Road dust	18.29	5.35	12.84	0.42	/	/	/	(Zhang et al., 2016)
Kumasi (West African)	Road dust	28.00	26.45	1.55	17.07	1.19	0.36	3.31	(Bandowe et al., 2019)
Xian	Road dust	36.53	31.01	5.52	5.62	2.75	2.77	0.99	(Wei et al., 2015)
Huainan	Road dust	27.11	25.9	1.21	21.40	0.59	0.27	2.19	(Liu et al., 2020)
Guwahati (India)	Road dust	21.50	0.80	20.70	0.16	/	/	/	(Hussain et al., 2015)
Wuhan	Road dust	3.50	1.29	2.21	0.85	0.17	2.04	0.09	(Liu et al., 2021)
New Delhi (India)	Dust-fall	61.63	56.5	5.13	11.01	/	/	/	(Mishra and Kulshrestha, 2017)
Xian	Dust-fall	14.6	7.4	7.2	1.03	/	/	/	（Han et al., 2009）
Huangshi	Dust-fall	36.61	25.15	11.46	2.19	/	/	/	（Zhan et al., 2016）
Nanchang	Dust-fall	24.46	15.18	9.28	1.64	/	/	/	(Zhang, 2014)
Beijing	Dust-fall	47.2	41.5	5.7	8.9	/	/	/	(Tang et al., 2013)
Tianjin	Road dust	13.17	10.63	2.54	4.05	/	/	/	(Ma et al., 2019)
Shijiazhuang	Road dust	20.65	18.34	2.29	5.83	/	/	/	(Guo et al., 2018)
Wuhu	Dust-fall	33.26	22.49	10.77	2.09	/	/	/	(Deng et al., 2014)
Xiaogan	Dust-fall	5.77	4.32	1.45	2.98	/	/	/	(Zhan et al., 2022)
Qaidam Basin	Dust-fall	3.27	1.88	1.41	3.66	1.14	0.25	4.97	This study

Line 438. It is confusing that this study focuses on PM larger than 10 μm, as the size cut for

dust sampling is not clearly stated. Biomass burning OA and EC are mainly in the PM2.5 size range.

Response:

Thank you for your valuable suggestions and feedback. The dust in this study was collected using a passive sampler. Over 90% of the collected dust particles were smaller than 100 μm, with approximately 25% less than 10 μm (Figure S16), indicating the presence of fine particles (<10 μm), albeit in a relatively small proportion. The particle size distribution of atmospheric dust deposition is similar to that of TSP, with both primarily consisting of particles smaller than 100 μm. Using PMF source apportionment, this study identified a notably high contribution from biomass burning in rural areas, particularly during the heating period. Similarly, studies on atmospheric TSP in Iran (Ashrafi et al., 2018), the Qinghai-Xizang Plateau (Lulang) (Zhao et al., 2013), Northeast China (Jia et al., 2024), and Qingdao (Liu et al., 2022) have also reported significant contributions from biomass and coal combustion. This suggests that contributions from biomass and coal combustion can indeed be observed in particles larger than 10 μm.

During the rural heating period, intensive biomass and coal burning for heating leads to substantial emissions of fine particles. Although initially emitted in the fine mode, these high concentrations of ultrafine particles can undergo coagulation or coalescence, aggregating with each other or onto pre-existing coarse particles, thereby increasing their overall size (Butler and Mulholland, 2004; Kulmala et al., 2004; Li et al., 2020). Furthermore, fine particles from biomass burning (e.g., carbonaceous materials) may mix internally with coarse particles such as soil dust or salt dust in the Qaidam Basin, forming internally mixed particles (Li et al., 2003; Hand et al., 2010). During source apportionment, such coarse, mixed particles are more likely to be attributed to the biomass burning source. Additionally, the Qaidam Basin is a significant source of salt dust (Zhu et al., 2025). Salt dust particles (e.g., halite, gypsum) provide excellent condensation nuclei for soluble substances emitted from biomass burning, considerably promoting hygroscopic growth (Li et al., 2003; Kumar, 2010; Wang, 2013). The basin's topography also favors the formation of stable inversion layers, which inhibit pollutant dispersion and allow particles more time to grow, mix, and age in the atmosphere. Prevailing wintertime winds may further transport pollutants from surrounding regions into the basin. Finally, the PMF model may have inherent uncertainties in resolving sources with similar chemical profiles. If the chemical compositions of local soil dust and biomass burning particles overlap after long-range transport and complex atmospheric reactions, the model may not fully separate them (Cesari et al., 2016). The relevant content has been added to the manuscript (**Lines 854-887**).

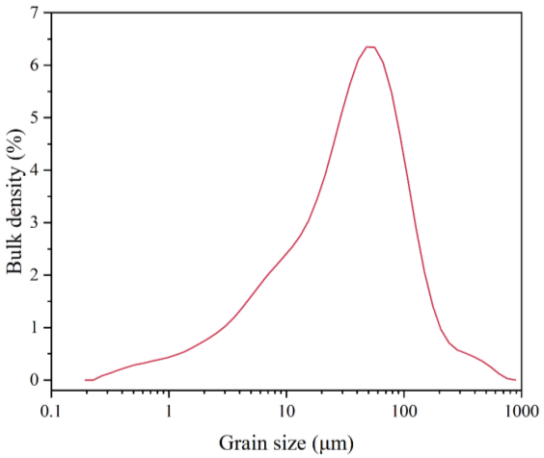

Figure S16 Particle size distribution characteristics of atmospheric dust-fall. This figure presents the results obtained from the particle size analysis of dust-fall samples collected in this study (Text S2).

Text S2.

Methods for the particle size analysis

The grain size of dust-fall samples was measured with a laser particle analyzer (Malvern Mastersizer 2000). The particle size distribution was calculated for 100 grain size classes within a measuring range of 0.02-2000 μm. Sample preparation for grain size analysis included wet oxidation of organic matter by adding 10 ml of 30% H_2O_2 per 1.5 g dry sample. Carbonates were dissolved by boiling with 10 ml (10% HCl) over 10 min. The glass beakers were filled up with 150 ml distilled water and suspended particles were left to deposit. After siphoning the supernatant water, 10 ml of 0.05 N $(NaPO_3)_6$ were added, and the residue was dispersed for 5 min in an ultrasonic bath before measurement (Lu and An, 1997). And the results are expressed as volume percentages.

Line 449. In the Method section (Line 223), soot EC is defined as EC1-OPC, which is very confusing. What about Ash EC (mentioned in Line 224)?

Response:

We apologize for the error in the manuscript, where the definitions were incorrectly stated. The correct definitions are: char-EC is defined as the difference between EC1 and OPC, and soot-EC is defined as the sum of EC2 and EC3. Relevant content has been revised in the manuscript (**Lines 236-240**). We will carefully review the entire manuscript to correct this and prevent similar errors from occurring again.

Line 475. When stating "supporting previous findings", please add references. Do these previous findings refer to the same site?

Response:

We sincerely apologize for any confusion caused by our oversight. The intended meaning was that the soot/char ratio results indicate carbon emissions in the Qaidam Basin primarily originate from

coal and biomass burning, which is consistent with the findings from the OC/EC ratio analysis, not a direct comparison with other studies. The sentence has been revised to (**Lines 517-519**): "This indicates that, in comparison to other regions, carbon emissions in the remote QDB are predominantly sourced from coal and biomass burning, supporting OC/EC ratio findings."

Line 483. This content is repetitive.

Response:
We agree with the reviewer and have deleted the sentence as suggested.

Line 485. Check the references—do they use MSR?

Response:
We apologize for the citation error. The calculation of SOC and POC in these two referred studies does not utilize the MSR method. This has been corrected in our manuscript.

Lines 527-528:
The MRS method enables discrimination of OC into POC and SOC (Method 2.7) (Yoo et al., 2022; Liu et al., 2023).

Line 516. Are you referring to Table S3 instead of Table S1?

Response:
We apologize for this oversight. Additional content has been incorporated into the supplementary file; accordingly, the table number has been updated to Table S5. The reference has been corrected to Table S5. We have double-checked the entire manuscript to prevent similar errors from occurring again.

Line 516. Why are the heavy metal levels lower in this study?

Response:
We really appreciate your review and suggestions. The low heavy metal content in dust deposition within the Qaidam Basin can be attributed to the following factors. The region has sparse human activity, lacks heavy industrial zones and dense urban clusters, resulting in low total anthropogenic emissions of heavy metals. Furthermore, the surface soil in the Qaidam Basin itself has a low background level of heavy metals, primarily derived from natural sources with relatively weak influence from human activities (Nuralykyzy et al., 2021; Chen et al., 2021). From the meteorological perspectives, the basin's high altitude, strong winds, and arid conditions with minimal precipitation favor the dispersion of atmospheric pollutants. This makes the formation of prolonged stagnant weather conditions unlikely, thereby preventing the accumulation of pollutants and the occurrence of high concentrations near the ground. A particularly unique aspect of the Qaidam Basin is its role as a significant source of salt dust. The recent study indicates that salt dust emitted from the playa lakes within the basin contributes substantially to atmospheric dust deposition (Zhu et al., 2025). These salt dust particles, composed mainly of soluble salts like NaCl

and gypsum, may dilute the relative concentration of non-salt components, such as heavy metals, when released into the atmosphere in large quantities. The combined effect of these factors leads to the observed low heavy metal content in dust deposition in this region. Relevant content has been added to the manuscript (**Lines 630-645**)

Line 523. You mentioned in Line 500 that coal combustion is more intense in rural areas, so these metal levels should be higher in rural areas rather than urban areas. Please clarify this inconsistency.

Response:
We greatly appreciate your feedback. This indicates that the seasonal variation in heavy metal concentrations in urban area, specifically the increase during the heating period compared to the non-heating period, may be attributed to elevated coal combustion for heating. In contrast, based on carbonaceous component analysis, rural areas exhibit more intensive coal usage than urban areas, yet the heavy metal content in atmospheric dust deposition is lower in rural regions. We attribute this discrepancy primarily to the following reasons. First, pollution sources in rural areas are relatively singular, whereas urban areas are influenced by more complex heavy metal sources. During the heating period, heavy metals in the rural atmosphere of the Qaidam Basin mainly originate from coal and biomass combustion. In contrast, urban areas are affected by a wider range of sources, including industrial activities, traffic emissions, and others (Liu et al., 2021; Huang et al., 2021a). Additionally, the dense building layout in urban areas hinders pollutant dispersion, leading to accumulation, while the open terrain in rural areas facilitates dilution and diffusion. This pattern, where rural heavy metal concentrations (particularly Pb, Cr, Cd, As, and other elements associated with coal combustion) are lower than those in urban areas during the heating season, has also been observed in studies conducted in Northeast China, Shanghai, Taiyuan, the Yangtze River Delta, and Southern Nigeria (Shi et al., 2012; Liu et al., 2021; Huang et al., 2021a; Liu et al., 2023b; Hilary et al., 2025). The relevant content has been added to the manuscript (**Lines 657-670**).

Line 553. Si and Al are trace elements, not ions—this classification is incorrect.

Response:
Sorry for the error caused by our negligence. The text in **Lines 731-732** has been revised to the following accurate description: "The second factor was identified as soil dust, characterized by trace elements such as Si (37.17%) and Al (29.18%), along with ions including nps-Cl^- (34.90%), nps-Mg^{2+} (28.21%), and Fe (24.43%) (Pervez et al., 2018; Tian et al., 2021)."

PMF results:

- Why was secondary formation only identified in Urban-NHP? Additionally, this attribution to secondary sources is highly problematic, as Figure S13 shows SOC was nearly 0 while POC was higher than SOC.

Response:
Thank you for your valuable suggestions and feedback. With the addition of supplementary content,

the PMF source apportionment result is now presented in Figure S14 (previously Figure S13). We suggest that the identification of a secondary aerosol source only during the NHP in urban areas can be attributed to several aspects. Firstly, dust deposition samples predominantly consist of larger particles, whereas the transformation into secondary particles typically occurs in sub-micron aerosols (Zhang et al., 2022b), making them less likely to be observed in deposition samples. Secondly, urban areas have higher emissions from industry and vehicles, leading to greater concentrations of precursor gases such as NOx and SO_2, which facilitates the formation of SIA compared to rural areas (Sandrini et al., 2016; Zhang et al., 2022b). Additionally, the NHP (generally May–September) is characterized by stronger solar radiation, higher temperatures, and increased relative humidity, all of which accelerate SIA formation (Pandolfi et al., 2010; Sandrini et al., 2016). Therefore, we consider the identification of a secondary aerosol source solely in urban-NHP to be reliable. From the perspective of PMF factor identification, only the urban-NHP factor showed high mass loadings of NO_3^- and nps-SO_4^{2-} (Liu et al., 2015; Liu et al., 2016). Contributions from other factors in this source profile were minimal, supporting its interpretation as a secondary aerosol source.

The identification of SIA in this factor, alongside zero contribution from secondary organic aerosol (SOA) but a detectable primary organic aerosol (POA) contribution, is reasonable and can be explained as follows. Firstly, carbon emissions during urban-NHP are lower than during Urban-HP, Rural-HP, and Rural-NHP. When emissions of organic compounds, particularly VOCs, are low, inorganic components may dominate the secondary aerosol factor (Qian et al., 2023). Studies also indicate that SIA can become physically mixed with certain POA types (e.g., from coal combustion or cooking) during transport, leading to high temporal correlation. This mixing may result in PMF identifying them as a single statistical factor. Furthermore, PMF resolves factors based on statistical covariance. The distinct chemical signatures of SIA (nitrate, sulfate) may allow clear separation, whereas SOA profiles might overlap with other sources or lack strong unique markers, making them difficult for PMF to resolve accurately (Liu et al., 2025). Additionally, the vehicle emission factor in the PMF solution already contains a high SOC contribution (65.05%). This can cause "factor competition" or source separation issues, potentially leading to an underestimation of SOC in other factors (Habre et al., 2011; Fossum et al., 2024). Since the POC factor does not exhibit this characteristic, it may explain why the secondary factor in urban-NHP shows a 3.18% POC contribution but 0% SOC. To more accurately reflect the chemical nature of this source, we have revised the term from "secondary aerosol" to "secondary inorganic aerosol" in the manuscript.

- Why does the salt lake factor have EC and SOC in its profile? As shown in Figure S13 for Rural-NHP, these should be 0.

Response:

Thank you for your insightful suggestions. We propose that the salt lake emission factor does not exist as an independent source. During atmospheric transport, it undergoes mixing with particles from various origins. Similar phenomena have been observed in source apportionment studies in Lanzhou (Zhang et al., 2022a) and Beijing (Yu et al., 2013; Srivastava et al., 2021), where salt lake-derived particles were found to be physically mixed with soil dust and soot from combustion processes during atmospheric transport. This implies that the factor resolved by PMF is not a single,

pure source but rather a mixed profile that co-varies in both time and space. Furthermore, the salt lake factor exhibits a high content of Cd. Given the presence of numerous salt lake resource development enterprises and mining vehicles around the Qaidam Basin's salt lakes, emissions from these activities may have mixed with the natural salt lake emissions. This mixing could explain the presence of Cd, along with SOC and EC, in the factor's source profile.

- As shown in Figure S13, the soil dust factor has nearly 40% SOC contribution for Rural-HP—why is this the case?

Response:

We apologize for the inaccuracies in the contribution of characteristic species in Figure S14. While the overall trend and identified factors remain unchanged, specific contribution values contained errors. Specifically, the SOC contribution of the soil dust factor in Rural-HP should be 27.52%. Contributions of SOC and EC were also present in the soil dust factors for Rural-NHP, Urban-HP, and Urban-NHP. Similar to the case of the salt lake source, we attribute this to mixing with combustion sources. Soil dust is not a purely mineral; it likely contains previously deposited combustion residues (e.g., from coal and biomass burning, and vehicle exhaust particles) (Srivastava et al., 2021; Liu et al., 2025). These residues inherently contain carbonaceous components, leading to the observed SOC contributions in the soil dust profile.

Line 561. Are these elements from internal combustion engines or traffic-induced road dust? I suspect it is the latter.

Response:

We greatly appreciate your feedback. This factor likely represents a mixture of vehicle exhaust and non-exhaust emissions (e.g., tire and brake wear, and resuspended road dust). Elements and ions primarily associated with exhaust emissions include V, NO_3^-, Ni, and carbonaceous components (Cong et al., 2011; Zhang et al., 2012). For instance, Ni can be emitted from fuel combustion and vehicle exhaust (Pacyna and Pacyna, 2001). In contrast, Cu, Zn, nps-Mg^{2+}, and nps-K^+ originate from non-exhaust vehicle emissions (brake and tire wear, and resuspended road dust) (Amato et al., 2014). For example, Zn may derive from rubber tire wear (Rogge et al., 1993), Pb emissions may be related to wear (tires/brakes) (Smichowski et al., 2007), and Cu is associated with brake wear (Lin et al., 2015). These results indicate that both exhaust and non-exhaust traffic emissions contribute to this factor. Quantifying the specific contributions of different non-exhaust emission types is challenging, as the concentrations of these metals vary based on numerous parameters, such as traffic flow and patterns, vehicle fleet characteristics, and local climate and geological conditions (Duong and Lee, 2011). Furthermore, the presence of crustal elements and ions like Fe, Si, and nps-Mg^{2+} in the traffic emission factor for Urban-NHP, Urban-HP, and Rural-NHP suggests an additional contribution from resuspended road dust (Chen et al., 2019). The corresponding text has been revised in the manuscript (**Lines 751-761**).

Line 669. Vehicle-road interactions should cause dust suspension (often defined as road dust), and this should contribute more than vehicle emissions.

Response:

We really appreciate your review and suggestions. Upon careful review, we recognize that the "Vehicle emission" factor represents a mixture of both exhaust and non-exhaust emissions (e.g., tire and brake wear, and resuspended road dust). Consequently, the description in **Lines 926-931** has been revised accordingly.

In addition to the distinctive energy consumption structure in the rural QDB, which leads to significant contributions from coal and biomass burning during HP, atmospheric dust deposition in the QDB during the NHP primarily originates from traffic and industrial emissions. The contribution from traffic emissions during the NHP was twice that during the HP. Considering the larger particle size of the dust samples collected in this study, the traffic-related dust is likely derived mainly from vehicle non-exhaust emissions, such as road dust (Gondwal and Mandal, 2021).

Figure 7a. How was Figure 7a generated? The PMF factor profiles in Figure S13 differ across different sites—please explain the integration process.

Response:

Thank you for your insightful suggestions. Figure 7a was generated through a systematic integration process. First, factors identified as representing the same source were extracted from the PMF factor profiles of each site (Urban and Rural) and heating season (HP and NHP) shown in Figure S14. Subsequently, the concentration percentages of the characteristic species (elements and ions) corresponding to each factor were arithmetically averaged to create a representative composite factor profile. Finally, species with an average contribution exceeding 20% in this composite profile were defined as characteristic markers of that source in atmospheric dust over the Qaidam Basin. Relative content has been added to the manuscript (**Lines 683-688**).

Figure 7b. Rename "Vehicle combustions" to "Vehicle". The term "Vehicle combustions" is inaccurate, as vehicles themselves are not burned.

Response:

We agree with the reviewer's suggestion and have renamed this factor to "Traffic emission" in the revised manuscript. We thank the reviewer for this valuable input.

Figure S4. Reorganize this figure by combining its subpanels into one layout that fits on a single page. Apply the same reorganization to Figure S5.

Response:

We sincerely apologize for any confusion caused by our oversight. Additional content has been incorporated into the supplementary file; accordingly, the figure number has been updated to Figure S5 and S6. We have resized Figures S5 and S6 and rearranged them into a single-page layout.

Figure S11. By definition, SOC+POC=OC and Soot-EC+Char-EC=total EC. The fractional contributions in this figure involve double counting of OC and EC, which is incorrect.

Response:

Sorry for the error caused by our negligence. Additional content has been incorporated into the supplementary file; accordingly, the figure number has been updated to Figure S12. The figure has been revised following a recalculation of the percentages, and the updated Figure S12 is presented below.

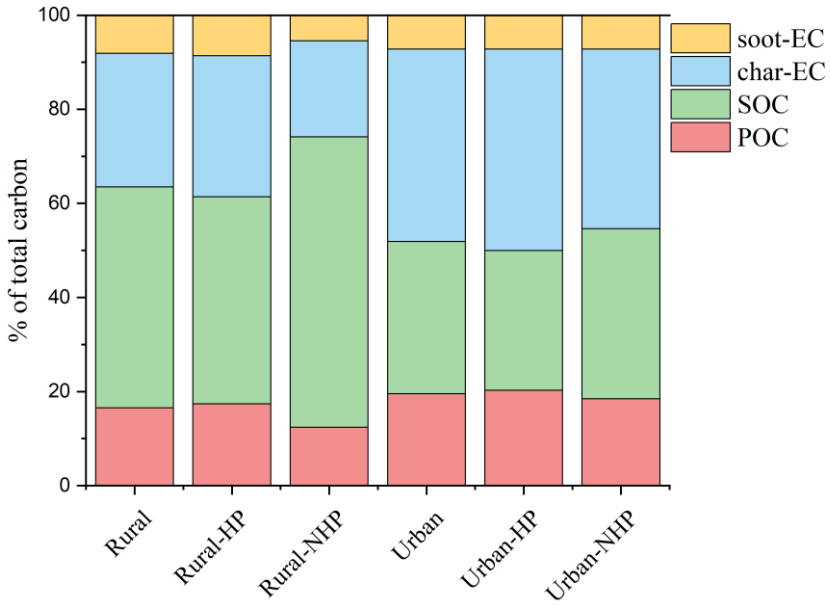

Figure S12 Proportions of various carbon indicators in urban and rural during heating and non-heating periods. [HP, domestic heating period; NHP, non-domestic heating period**].**

Table S2. It is impossible for PMF to have 0% uncertainty—this value is erroneous and needs correction.

Response:

We greatly appreciate your feedback. The uncertainty in Table S2 refers to the "Extra Modeling Uncertainty". In our PMF analysis, the "Extra Modeling Uncertainty" parameter was set to 0%, meaning that no additional uncertainty beyond the base level was introduced during the source apportionment process. The PMF model allows users to assign an extra modeling uncertainty for each observational data point (i.e., per chemical species per sample). This value, combined with the base uncertainty, which is generally derived from analytical parameters such as the method detection limit or measurement precision, affects the weighting of the data point in the model fitting. In the present study, the input dataset was configured without incorporating any extra modeling uncertainty. We agree that including this value in the main table was not appropriate. It has been removed from the table and instead documented as an input parameter in Text S1 of the Supplementary file.

Table S3. Provide mean values instead of ranges to facilitate better comparison.

Response:

Thank you for your valuable suggestions and feedback. Additional content has been incorporated into the supplementary file. Accordingly, the table number has been updated to Table S5. We have

revised the presentation of heavy metal concentrations in Table S5, standardizing the comparison by using mean values.

Table S5 Comparison of dust-fall metal concentrations in this study with those from other regions.

City	Country	Element					Reference
		Cd	Cr	Cu	Pb	Zn	
Guangzhou	China	4.22±1.21	62.2±27.1	116±30	72.6±17.9	504±191	Cai et al., 2013
Xi'an	China	4.18±1.20	195.92±48.66	125.31±78.80	310.29±80.79	721.20±237.57	Chen et al., 2017
Suzhou	China	2.45±4.89	25.7±15.4	104.8±214.9	262.2±494.4	376.9±712.4	Ma et al., 2016
Changsha	China	9.11	80.7	43.9	66.6	215	Li et al., 2016
Beijing	China	0.72±0.74	84.7±30.8	69.9±68.3	105±223	222±120	Wei et al., 2015
Tianjin	China	0.45	71.85	55.47	254	–	Yu et al., 2014
Huainan	China	0.25	61.1	36.3	42.6	–	Tang et al., 2017
Shanghai	China	1.23	159.3	196.8	294.9	733.8	Shi et al., 2008
Lanzhou	China	0.81±0.72	96.9±54.6	77.4±19.8	34.7±12.2	56.6±40.6	Jiang et al., 2018
Jinan	China	0.24	135.95	–	110.78	380.22	Pang et al., 2014
Galicia	Spain	0.31±0.13	54.1±10.8	20.5±11.3	11.7±33.1	98.7±71.3	Franco-Uria et al., 2009
Alexandria	Egypt	0.33	24.3	79.7	70.3	169	Dat et al., 2021
Ho Chi Minh City,	Vietnam	0.5	102.4	153.7	49.6	466.4	Jadoon et al., 2021
Cantabria region	Spain	0.1	5.2	11.8	4.5	183	Fernandez-Olmo et al., 2015
Junggar Basin	China	16.65	605.5	100.1	–	5933.9	(Yang et al., 2016)
Ebinur Basin	China	0.34±0.037	102.17±3.57	24.52±3.11	16.32±1.02	157.16±5.14	(Abuduwailil et al., 2015)
Qaidam Basin	China	0.47±0.45	7.38±6.90	8.12±6.82	14.82±14.23	58.47±52.05	This study

Figure S13. Reorganize this figure to improve readability, as it currently spans 4 pages. In addition to factor profiles, can you provide time series of factor contributions? Note that the left y-axis is labeled "concentration of species", but factor profiles are normalized values, not actual concentrations—this mislabeling should be fixed.

Response:

Thank you for your insightful suggestions. Additional content has been incorporated into the supplementary file; accordingly, the figure number has been updated to Figure S14. We have redesigned the layout of Figure S14 and added a time-series plot (Figure S15). Based on these updates, relevant discussion has been incorporated into the manuscript. It should be noted that the data were not normalized during the PMF source apportionment analysis; thus, the left y-axis represents the actual species concentration.

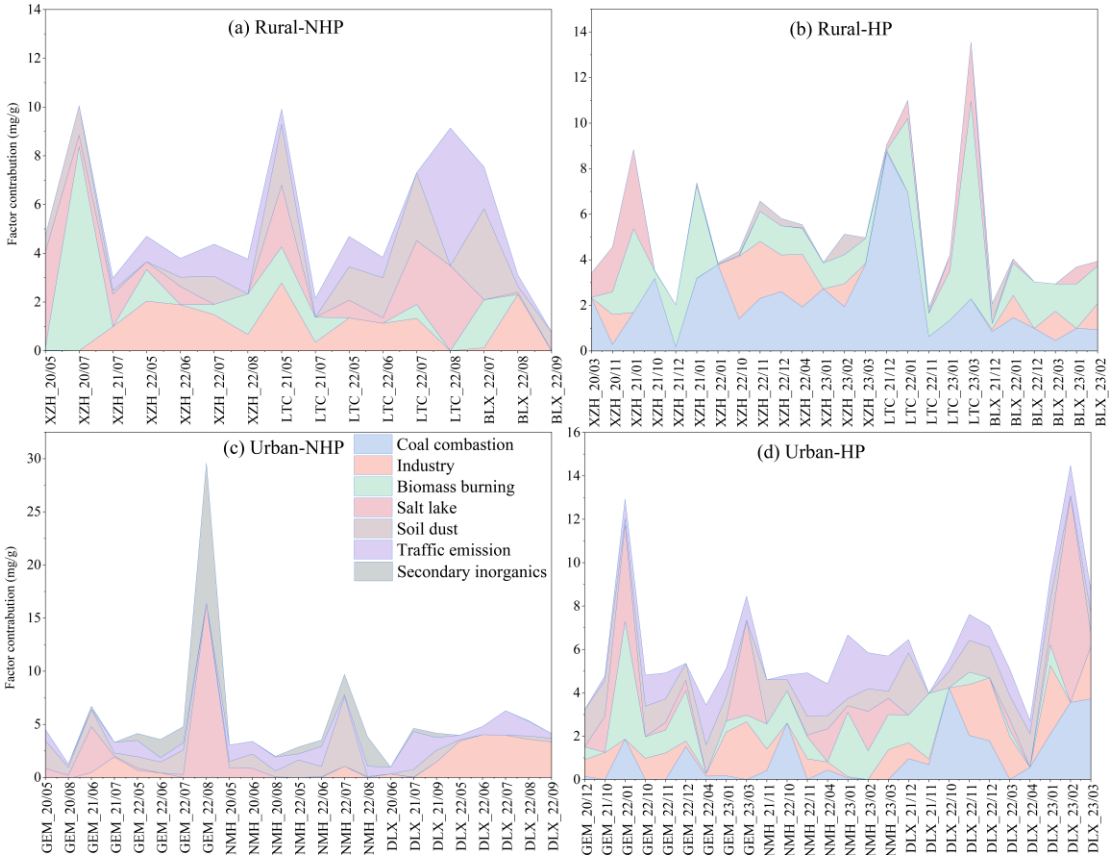

Figure S15 Temporal variations in factor contributions to atmospheric dust deposition in the Qaidam Basin: (a) Rural NHP, (b) Rural HP, (c) Urban NHP, and (d) Urban HP. HP, domestic heating period; NHP, non-domestic heating period.

Lines 705-707:

Salt lake emissions were most pronounced in rural areas during the HP of 2023 at site LTC and during the NHP of 2020 at site XZH. In urban areas, elevated contributions occurred during the NHP and HP of 2022 at site GEM, and during the HP of 2023 at site DLX.

Lines 735-737:

The temporal variation of soil dust was largely consistent with that of the salt lake source, indicating the fact that they may be influenced by similar factors.

Lines 761-764:

For traffic emissions during the NHP, peaks were observed in both rural and urban areas in 2022,

generally concentrated in July, August, and September, coinciding with the tourism high season. During the HP, traffic emissions primarily occurred in 2021 at GEM and in 2023 at DLX.

Lines 784-785:

Coal combustion was more intense at site LTC in rural areas and at site DLX in urban areas.

Lines 797-799:

Biomass burning made significant contributions in urban areas in 2021 and 2022. In rural areas, biomass burning emissions were particularly strong, especially during the HP at LTC and the NHP at XZH.

Lines 814-815:

Industrial emissions showed greater contributions during the HP at XZH and at DLX.

Lines 836-842:

The secondary inorganic aerosol source was identified only in Urban-NHP, peaking in August 2022 at GEM and in June, July, and August 2022 at NMH. This trend closely followed the distribution of traffic emissions, suggesting that the formation of secondary aerosols is linked to increased traffic activity. Traffic emissions, particularly vehicle exhaust, are a significant source of secondary inorganic aerosols (especially nitrate) in urban atmospheres (Ma et al., 2017). Source apportionment studies in Beijing have similarly found that the contribution of secondary inorganic aerosols increases in summer, closely associated with traffic emissions (Zhang et al., 2013).

Reference

Abdollahi, S., Karimi, A., Madadi, M., Eslamian, S., Ostad-Ali-Askari, K., and Singh, V. P.: Lead concentration in dust fall in Zahedan, Sistan and Baluchistan Province, Iran, Journal of Geography and Cartography, 4, 6, 10.24294/jgc.v4i2.601, 2021.

Adeniran, J. A., Yusuf, R. O., and Olajire, A. A.: Exposure to coarse and fine particulate matter at and around major intra-urban traffic intersections of Ilorin metropolis, Nigeria, Atmospheric Environment, 166, 383-392, 10.1016/j.atmosenv.2017.07.041, 2017.

Almeida, S. M., Lage, J., Fernández, B., Garcia, S., Reis, M. A., and Chaves, P. C.: Chemical characterization of atmospheric particles and source apportionment in the vicinity of a steelmaking industry, Science of The Total Environment, 521-522, 411-420, https://doi.org/10.1016/j.scitotenv.2015.03.112, 2015.

Alzahrani, A. J., Alghamdi, A. G., and Ibrahim, H. M.: Assessment of soil loss due to wind erosion and dust deposition: Implications for sustainable management in arid regions, Applied Sciences, 14(23), 10822, 10.3390/app142310822, 2024.

An, L., Che, H., Xue, M., Zhang, T., Wang, H., Wang, Y., Zhou, C., Zhao, H., Gui, K., Zheng, Y., Sun, T., Liang, Y., Sun, E., Zhang, H., and Zhang, X.: Temporal and spatial variations in sand and dust storm events in East Asia from 2007 to 2016: Relationships with surface conditions and climate change, Science of The Total Environment, 633, 452-462, https://doi.org/10.1016/j.scitotenv.2018.03.068, 2018.

Ashrafi, K., Fallah, R., Hadei, M., Yarahmadi, M., and Shahsavani, A.: Source apportionment of Total Suspended Particles (TSP) by Positive Matrix Factorization (PMF) and Chemical Mass

Balance (CMB) modeling in Ahvaz, Iran, Archives of Environmental Contamination and Toxicology, 75, 278-294, 10.1007/s00244-017-0500-z, 2018.

Barjoee, S. S., Abadi, S. Z. M., Elmi, M. R., Varaoon, V. T., and Nikbakht, M.: Evaluation of trace elements pollution in deposited dust on residential areas and agricultural lands around Pb/Zn mineral areas using modified pollution indices, Journal of Environmental Health Science and Engineering, 19, 753-769, 10.1007/s40201-021-00643-8, 2021.

Brown, S. G., Eberly, S., Paatero, P., and Norris, G. A.: Methods for estimating uncertainty in PMF solutions: examples with ambient air and water quality data and guidance on reporting PMF results, Science of The Total Environment, 518-519, 626-635, 10.1016/j.scitotenv.2015.01.022, 2015.

Butler, K. M. and Mulholland, G. W.: Generation and transport of smoke components, Fire Technology, 40, 149-176, 10.1023/B:FIRE.0000016841.07530.64, 2004.

Cesari, D., Amato, F., Pandolfi, M., Alastuey, A., Querol, X., and Contini, D.: An inter-comparison of PM10 source apportionment using PCA and PMF receptor models in three European sites, Environmental Science and Pollution Research, 23, 15133-15148, 10.1007/s11356-016-6599-z, 2016.

Chen, L., Zhang, X.-Y., Tang, Q.-L., Geng, J., Wang, E.-L., and Li, J.-Y.: Heavy metal pollution and source analysis in surface soil of the Qaidam Basin, Environmental Science, 42, 4880-4888, https://doi.org/10.13227/j.hjkx.202101052, 2021.

Chow, J. C.: Measurement methods to determine compliance with ambient air quality standards for suspended particles, Journal of the Air & Waste Management Association, 45, 320-382, 10.1080/10473289.1995.10467369, 1995.

Fossum, K. N., Lin, C., O'Sullivan, N., Lei, L., Hellebust, S., Ceburnis, D., Afzal, A., Tremper, A., Green, D., Jain, S., Byčenkienė, S., O'Dowd, C., Wenger, J., and Ovadnevaite, J.: Two distinct ship emission profiles for organic-sulfate source apportionment of PM in sulfur emission control areas, Atmospheric Chemistry and Physics, 24, 10815-10831, 10.5194/acp-24-10815-2024, 2024.

Goossens, D. and Offer, Z. Y. J. Z. F. G.: Eolian deposition of dust over symmetrical hills: an evaluation of wind-tunnel data by means of terrain measurement, 37, 103-111, 1993.

Habre, R., Coull, B., and Koutrakis, P.: Impact of source collinearity in simulated $PM_{2.5}$ data on the PMF receptor model solution, Atmospheric Environment, 45, 6938-6946, https://doi.org/10.1016/j.atmosenv.2011.09.034, 2011.

Han, Y., Cao, J., An, Z., Chow, J. C., Watson, J. G., Jin, Z., Fung, K., and Liu, S.: Evaluation of the thermal/optical reflectance method for quantification of elemental carbon in sediments, Chemosphere, 69, 526-533, 10.1016/j.chemosphere.2007.03.035, 2007.

Han, Y. M., Cao, J. J., Chow, J. C., Watson, J. G., An, Z. S., and Liu, S. X.: Elemental carbon in urban soils and road dusts in Xi'an, China and its implication for air pollution, Atmospheric Environment, 43, 2464-2470, https://doi.org/10.1016/j.atmosenv.2009.01.040, 2009.

Han, Y. M., Cao, J. J., Yan, B. Z., Kenna, T. C., Jin, Z. D., Cheng, Y., Chow, J. C., and An, Z. S.: Comparison of Elemental Carbon in Lake Sediments Measured by Three Different Methods and 150-Year Pollution History in Eastern China, Environmental Science & Technology, 45, 5287-5293, 10.1021/es103518c, 2011.

Hand, V. L., Capes, G., Vaughan, D. J., Formenti, P., Haywood, J. M., and Coe, H.: Evidence of internal mixing of African dust and biomass burning particles by individual particle analysis

using electron beam techniques, Journal of Geophysical Research: Atmospheres, 115, https://doi.org/10.1029/2009JD012938, 2010.

Harrison, R. M., Smith, D. J. T., Piou, C. A., and Castro, L. M.: Comparative receptor modelling study of airborne particulate pollutants in Birmingham (United Kingdom), Coimbra (Portugal) and Lahore (Pakistan), Atmospheric Environment, 31, 3309-3321, https://doi.org/10.1016/S1352-2310(97)00152-0, 1997.

Hilary, U., Efeoghene, E. A., Issac, A. O., Sami, R., Baakdah, F., and Pareek, S.: Exposure to airborne pollutants in urban and rural areas: levels of metals and microorganisms in PM10 and gaseous pollutants in ambient air, Air Quality, Atmosphere & Health, 18, 317-332, 10.1007/s11869-024-01644-w, 2025.

Huang, H., Xu, Z.-Q., Yan, J.-X., Zhao, X.-G., and Wang, D.-L.: Characteristics of Heavy Metal Pollution and Ecological Risk Evaluation of Indoor Dust from Urban and Rural Areas in Taiyuan City During the Heating Season, Journal of Environmental Science, 42, 2143-2152, 10.13227/j.hjkx.202008045, 2021.

Ji, X., Xu, K., Liao, D., Chen, G., Liu, T., Hong, Y., Dong, S., Choi, S.-D., and Chen, J.: Spatial-temporal characteristics and source apportionment of ambient VOCs in Southeast Mountain Area of China, Aerosol and Air Quality Research, 22, 220016, 10.4209/aaqr.220016, 2022.

Jia, S.-M., Chen, M.-H., Yang, P.-F., Wang, L., Wang, G.-Y., Liu, L.-Y., and Ma, W.-L.: Seasonal variations and sources of atmospheric EPFRs in a megacity in severe cold region: Implications for the influence of strong coal and biomass combustion, Environmental Research, 252, 10.1016/j.envres.2024.119067, 2024.

Jun Li, J., Ge, H. W., Xin, M. W., Jun, J. C., Tao, S., Chun, L. C., Jing, J. M., A., F. H. T., and Xin Liu, s.: Abundance, composition and source of atmospheric $PM_{2.5}$ at a remote site in the Tibetan Plateau, China, Tellus B: Chemical and Physical Meteorology, 65, 20281, 10.3402/tellusb.v65i0.20281, 2013.

Khan, A. J., Swami, K., Ahmed, T., Bari, A., Shareef, A., and Husain, L.: Determination of elemental carbon in lake sediments using a thermal–optical transmittance (TOT) method, Atmospheric Environment, 43, 5989-5995, https://doi.org/10.1016/j.atmosenv.2009.08.030, 2009.

Kocbach Bølling, A., Pagels, J., Yttri, K. E., Barregard, L., Sallsten, G., Schwarze, P. E., and Boman, C.: Health effects of residential wood smoke particles: the importance of combustion conditions and physicochemical particle properties, Particle and Fibre Toxicology, 6, 29, 10.1186/1743-8977-6-29, 2009.

Kulmala, M., Vehkamäki, H., Petäjä, T., Dal Maso, M., Lauri, A., Kerminen, V. M., Birmili, W., and McMurry, P. H.: Formation and growth rates of ultrafine atmospheric particles: a review of observations, Journal of Aerosol Science, 35, 143-176, https://doi.org/10.1016/j.jaerosci.2003.10.003, 2004.

Kumar, A.: Chemical characterization of mineral aerosols: Sources, transport and atmospheric transformations, Mohanlal Sukhadia University Udaipur, 2010.

Li, J., Pósfai, M., Hobbs, P. V., and Buseck, P. R.: Individual aerosol particles from biomass burning in southern Africa: 2, Compositions and aging of inorganic particles, Journal of Geophysical Research: Atmospheres, 108, https://doi.org/10.1029/2002JD002310, 2003.

Li, J., Teng, [Initial], Wu, J., Chen, H.-Y., and Jiang, J.-Y.: Uncertainty in source analysis of soil heavy metals using PMF model, China Environmental Science, 40, 716-725, 2020.

Li, R., Li, C., Zhuang, J., Zhu, H., Fang, L., and Sun, D.: Mechanistic influence of chemical

agglomeration agents on removal of inhalable particles from coal combustion, ACS Omega, 5, 25906-25912, 10.1021/acsomega.0c03263, 2020.

Lin, Y. C., Tsai, C. J., Wu, Y. C., Zhang, R., Chi, K. H., Huang, Y. T., Lin, S. H., and Hsu, S. C.: Characteristics of trace metals in traffic-derived particles in Hsuehshan Tunnel, Taiwan: size distribution, potential source, and fingerprinting metal ratio, Atmospheric Chemistry and Physics, 15, 4117-4130, 10.5194/acp-15-4117-2015, 2015.

Liu, B., Song, N., Dai, Q., Mei, R., Sui, B., Bi, X., and Feng, Y.: Chemical composition and source apportionment of ambient PM2.5 during the non-heating period in Taian, China, Atmospheric Research, 170, 23-33, 10.1016/j.atmosres.2015.11.002, 2016.

Liu, G., Li, J., Wu, D., and Xu, H.: Chemical composition and source apportionment of the ambient $PM_{2.5}$ in Hangzhou, China, Particuology, 18, 135-143, https://doi.org/10.1016/j.partic.2014.03.011, 2015.

Liu, H., Jia, M., Tao, J., Yao, D., Li, J., Zhang, R., Li, L., Xu, M., Fan, Y., Liu, Y., and Cheng, K.: Elucidating pollution characteristics, temporal variation and source origins of carbonaceous species in Xinxiang, a heavily polluted city in North China, Atmospheric Environment, 298, 119626, https://doi.org/10.1016/j.atmosenv.2023.119626, 2023a.

Liu, T., Zhao, C., Chen, Q., Li, L., Si, G., Li, L., and Guo, B.: Characteristics and health risk assessment of heavy metal pollution in atmospheric particulate matter in different regions of the Yellow River Delta in China, Environmental Geochemistry and Health, 45, 2013-2030, 10.1007/s10653-022-01318-5, 2023b.

Liu, X., Wang, Y., Liu, R., Zhang, Y., Shao, L., Han, K., and Zhang, Y.: Pollution characteristics, source identification and potential ecological risk of 50 elements in atmospheric particulate matter during winter in Qingdao, Arabian Journal of Geosciences, 15, 10.1007/s12517-022-09521-5, 2022.

Liu, X., Zhang, X., Jin, B., Wang, T., Qian, S., Zou, J., Dinh, V. N. T., Jaffrezo, J.-L., Uzu, G., Dominutti, P., Darfeuil, S., Favez, O., Conil, S., Marchand, N., Castillo, S., de la Rosa, J. D., Grange, S., Hueglin, C., Eleftheriadis, K., Diapouli, E., Manousakas, M.-I., Gini, M., Nava, S., Calzolai, G., Alves, C., Monge, M., Reche, C., Harrison, R. M., Hopke, P. K., Alastuey, A., and Querol, X.: Source apportionment of PM_{10} based on offline chemical speciation data at 24 European sites, npj Climate and Atmospheric Science, 8, 255, 10.1038/s41612-025-01097-7, 2025.

Liu, Y., Hu, J., Wang, X., Jia, J., Li, J., Wang, L., Hao, L., and Gao, P.: Distribution, bioaccessibility, and health risk assessment of heavy metals in $PM_{2.5}$ and PM_{10} during winter heating periods in five types of cities in Northeast China, Ecotoxicology and Environmental Safety, 214, 112071, https://doi.org/10.1016/j.ecoenv.2021.112071, 2021.

Manousakas, M., Papaefthymiou, H., Diapouli, E., Migliori, A., Karydas, A. G., Bogdanovic-Radovic, I., and Eleftheriadis, K.: Assessment of $PM_{2.5}$ sources and their corresponding level of uncertainty in a coastal urban area using EPA PMF 5.0 enhanced diagnostics, Science of The Total Environment, 574, 155-164, 10.1016/j.scitotenv.2016.09.047, 2017.

Millet, D. B., Donahue, N. M., Pandis, S. N., Polidori, A., Stanier, C. O., Turpin, B. J., and Goldstein, A. H.: Atmospheric volatile organic compound measurements during the Pittsburgh Air Quality Study: Results, interpretation, and quantification of primary and secondary contributions, Journal of Geophysical Research: Atmospheres, 110, https://doi.org/10.1029/2004JD004601, 2005.

Nuralykyzy, B., Wang, P., Deng, X., An, S., and Huang, Y.: Heavy metal contents and assessment of soil contamination in different land-use types in the Qaidam Basin, 10.3390/su132112020, 2021.

Offer, Z. Y., Goossens, D., and Shachak, M.: Aeolian deposition of nitrogen to sandy and loessial ecosystems in the Negev Desert, Journal of Arid Environments, 23, 355-363, https://doi.org/10.1016/S0140-1963(18)30609-8, 1992.

Paatero, P., Eberly, S., Brown, S. G., and Norris, G. A.: Methods for estimating uncertainty in factor analytic solutions, Atmospheric Measurement Techniques, 7, 781-797, 10.5194/amt-7-781-2014, 2014.

Pandolfi, M., Gonzalez-Castanedo, Y., Alastuey, A., de la Rosa, J. D., Mantilla, E., de la Campa, A. S., Querol, X., Pey, J., Amato, F., and Moreno, T.: Source apportionment of PM_{10} and $PM_{2.5}$ at multiple sites in the strait of Gibraltar by PMF: impact of shipping emissions, Environmental Science and Pollution Research, 18, 260-269, 10.1007/s11356-010-0373-4, 2010.

Pervez, S., Bano, S., Watson, J. G., Chow, J. C., Matawle, J. L., Shrivastava, A., Tiwari, S., and Pervez, Y. F.: Source profiles for $PM_{10\text{-}2.5}$ resuspended dust and vehicle exhaust emissions in Central India, Aerosol and Air Quality Research, 18, 1660-1672, 10.4209/aaqr.2017.08.0259, 2018.

Pipal, A. S., Singh, S., and Satsangi, G. P.: Study on bulk to single particle analysis of atmospheric aerosols at urban region, Urban Climate, 27, 243-258, https://doi.org/10.1016/j.uclim.2018.12.008, 2019.

Putaud, J.-P., Van Dingenen, R., Baltensperger, U., Brüggemann, E., Charron, A., Facchini, M. C., Decesari, S., Fuzzi, S., Gehrig, R., and Hansson, H.-C.: A European Aerosol Phenomenology: physical and chemical characteristics of particulate matter at kerbside, urban, rural and background sites in Europe, 2003.

Qian, Y., Cai, D., Zhang, M., Huang, X., Huo, J., Duan, Y., and Cheng, T.: Chemical composition, sources and evolution of wintertime inorganic and organic aerosols in urban Shanghai, China, 11 - 2023, 10.3389/fenvs.2023.1199652, 2023.

Qiu, Y., Wu, Z., Man, R., Zong, T., Liu, Y., Meng, X., Chen, J., Chen, S., Yang, S., Yuan, B., Song, M., Kim, C., Ahn, J., Zeng, L., Lee, J., and Hu, M.: Secondary aerosol formation drives atmospheric particulate matter pollution over megacities (Beijing and Seoul) in East Asia, Atmospheric Environment, 301, 119702, https://doi.org/10.1016/j.atmosenv.2023.119702, 2023.

Rastogi, N. and Sarin, M. M.: Quantitative chemical composition and characteristics of aerosols over western India: One-year record of temporal variability, Atmospheric Environment, 43, 3481-3488, https://doi.org/10.1016/j.atmosenv.2009.04.030, 2009.

Sandrini, S., van Pinxteren, D., Giulianelli, L., Herrmann, H., Poulain, L., Facchini, M. C., Gilardoni, S., Rinaldi, M., Paglione, M., Turpin, B. J., Pollini, F., Bucci, S., Zanca, N., and Decesari, S.: Size-resolved aerosol composition at an urban and a rural site in the Po Valley in summertime: implications for secondary aerosol formation, Atmospheric Chemistry and Physics, 16, 10879-10897, 10.5194/acp-16-10879-2016, 2016.

Sandrini, S., Fuzzi, S., Piazzalunga, A., Prati, P., Bonasoni, P., Cavalli, F., Bove, M. C., Calvello, M., Cappelletti, D., Colombi, C., Contini, D., de Gennaro, G., Di Gilio, A., Fermo, P., Ferrero, L., Gianelle, V., Giugliano, M., Ielpo, P., Lonati, G., Marinoni, A., Massabò, D., Molteni, U., Moroni, B., Pavese, G., Perrino, C., Perrone, M. G., Perrone, M. R., Putaud, J.-P., Sargolini, T.,

Vecchi, R., and Gilardoni, S.: Spatial and seasonal variability of carbonaceous aerosol across Italy, Atmospheric Environment, 99, 587-598, https://doi.org/10.1016/j.atmosenv.2014.10.032, 2014.

Sheoran, R., Dumka, U. C., Kaskaoutis, D. G., Grivas, G., Ram, K., Prakash, J., Hooda, R. K., Tiwari, R. K., and Mihalopoulos, N.: Chemical composition and source apportionment of total suspended particulate in the Central Himalayan Region, 10.3390/atmos12091228, 2021.

Shi, G., Chen, Z., Teng, J., Bi, C., Zhou, D., Sun, C., Li, Y., and Xu, S.: Fluxes, variability and sources of cadmium, lead, arsenic and mercury in dry atmospheric depositions in urban, suburban and rural areas, Environmental Research, 113, 28-32, https://doi.org/10.1016/j.envres.2012.01.001, 2012.

Simoneit, B. R. T.: Biomass burning — a review of organic tracers for smoke from incomplete combustion, Applied Geochemistry, 17, 129-162, https://doi.org/10.1016/S0883-2927(01)00061-0, 2002.

Smichowski, P., Gómez, D., Frazzoli, C., and Caroli, S.: Traffic - related elements in airborne particulate matter, Applied Spectroscopy Reviews, 43, 23-49, 10.1080/05704920701645886, 2007.

Smith, R. M. and Twiss, P. C.: Extensive gaging of dust deposition rates, 68:2, 10.2307/3626489

Journal Name: Kansas Acad. Sci; (United States); Journal Volume: 68:2, 1965.

Srivastava, D., Xu, J., Vu, T. V., Liu, D., Li, L., Fu, P., Hou, S., Moreno Palmerola, N., Shi, Z., and Harrison, R. M.: Insight into $PM_{2.5}$ sources by applying positive matrix factorization (PMF) at urban and rural sites of Beijing, Atmospheric Chemistry and Physics, 21, 14703-14724, 10.5194/acp-21-14703-2021, 2021.

Sulong, N. A., Latif, M. T., Sahani, M., Khan, M. F., Fadzil, M. F., Tahir, N. M., Mohamad, N., Sakai, N., Fujii, Y., Othman, M., and Tohno, S.: Distribution, sources and potential health risks of polycyclic aromatic hydrocarbons (PAHs) in $PM_{2.5}$ collected during different monsoon seasons and haze episode in Kuala Lumpur, Chemosphere, 219, 1-14, 10.1016/j.chemosphere.2018.11.195, 2019.

Tian, M., Gao, J., Zhang, L., Zhang, H., Feng, C., and Jia, X.: Effects of dust emissions from wind erosion of soil on ambient air quality, Atmospheric Pollution Research, 12, 10.1016/j.apr.2021.101108, 2021.

Torres, A., Bond, T. C., Lehmann, C. M. B., Subramanian, R., and Hadley, O. L.: Measuring organic carbon and black carbon in rainwater: Evaluation of methods, Aerosol Science and Technology, 48, 239-250, 10.1080/02786826.2013.868596, 2014.

Wang, F.: The mechanism and timescales of soil formation in the hyper-arid Atacama Desert, Chile, Purdue University, 2013.

Wang, M., Duan, Y., Xu, W., Wang, Q., Zhang, Z., Yuan, Q., Li, X., Han, S., Tong, H., Huo, J., Chen, J., Gao, S., Wu, Z., Cui, L., Huang, Y., Xiu, G., Cao, J., Fu, Q., and Lee, S.: Measurement report: Characterisation and sources of the secondary organic carbon in a Chinese megacity over 5 years from 2016 to 2020, Atmospheric Chemistry and Physics, 22, 12789-12802, 10.5194/acp-22-12789-2022, 2022.

Wei, N., Ma, C., Liu, J., Wang, G., Liu, W., Zhuoga, D., Xiao, D., and Yao, J.: Size-segregated characteristics of carbonaceous aerosols during the monsoon and non-monsoon seasons in Lhasa in the Tibetan Plateau, 10.3390/atmos10030157, 2019.

Wu, C. and Yu, J. Z.: Determination of primary combustion source organic carbon-to-elemental

carbon (OC/EC) ratio using ambient OC and EC measurements: secondary OC-EC correlation minimization method, Atmospheric Chemistry and Physics, 16, 5453-5465, 10.5194/acp-16-5453-2016, 2016.

Wu, C., Wu, D., and Yu, J. Z.: Quantifying black carbon light absorption enhancement with a novel statistical approach, Atmospheric Chemistry and Physics, 18, 289-309, 10.5194/acp-18-289-2018, 2018a.

Wu, G., Wan, X., Gao, S., Fu, P., Yin, Y., Li, G., Zhang, G., Kang, S., Ram, K., and Cong, Z.: Humic-Like Substances (HULIS) in aerosols of Central Tibetan Plateau (Nam Co, 4730 m asl): Abundance, light absorption properties, and sources, Environmental Science & Technology, 52, 7203-7211, 10.1021/acs.est.8b01251, 2018b.

Xiang, Y., Li, X., Zhang, T., Cheng, Q., Yan, C., Liu, X., Liu, Y., Wang, Y., Kang, S., Ding, X., and Zheng, M.: Characteristics and sources of organic aerosol in $PM_{2.5}$ at Yangbajing in Tibetan Plateau, Atmospheric Environment, 333, 120662, https://doi.org/10.1016/j.atmosenv.2024.120662, 2024.

Yan, B., Zheng, M., Hu, Y., Ding, X., Sullivan, A. P., Weber, R. J., Baek, J., Edgerton, E. S., and Russell, A. G.: Roadside, urban, and rural comparison of Primary and Secondary Organic molecular markers in ambient $PM_{2.5}$, Environmental Science & Technology, 43, 4287-4293, 10.1021/es900316g, 2009.

Yang, X., Zhou, C., Huo, W., Yang, F., Liu, X., and Mamtimin, A.: A study on the effects of soil moisture, air humidity, and air temperature on wind speed threshold for dust emissions in the Taklimakan Desert, Natural Hazards, 97, 1069-1081, 10.1007/s11069-019-03686-1, 2019.

Yao, L., Yang, L., Yuan, Q., Yan, C., Dong, C., Meng, C., Sui, X., Yang, F., Lu, Y., and Wang, W.: Sources apportionment of $PM_{2.5}$ in a background site in the North China Plain, Science of The Total Environment, 541, 590-598, https://doi.org/10.1016/j.scitotenv.2015.09.123, 2016.

Yu, L., Wang, G., Zhang, R., Zhang, L., Song, Y., Wu, B., Li, X., An, K., and Chu, J.: Characterization and source apportionment of $PM_{2.5}$ in an urban environment in Beijing, Aerosol and Air Quality Research, 13, 574-583, 10.4209/aaqr.2012.07.0192, 2013.

Zhan, C., Han, Y., Cao, J., Wei, C., Zhang, J., and An, Z.: Validation and application of a thermal–optical reflectance (TOR) method for measuring black carbon in loess sediments, Chemosphere, 91, 1462-1470, https://doi.org/10.1016/j.chemosphere.2012.12.011, 2013.

Zhang, M., Jia, J., Wang, B., Zhang, W., Gu, C., Zhang, X., and Zhao, Y.: Source apportionment of fine particulate matter during the day and night in Lanzhou, NW China, 10.3390/ijerph19127091, 2022a.

Zhang, N., Cao, J., Ho, K., and He, Y.: Chemical characterization of aerosol collected at Mt. Yulong in wintertime on the southeastern Tibetan Plateau, Atmospheric Research, 107, 76-85, https://doi.org/10.1016/j.atmosres.2011.12.012, 2012.

Zhang, N., Cao, J., Liu, S., Zhao, Z., Xu, H., and Xiao, S.: Chemical composition and sources of PM2.5 and TSP collected at Qinghai Lake during summertime, Atmospheric Research, 138, 213-222, https://doi.org/10.1016/j.atmosres.2013.11.016, 2014.

Zhang, X., Wang, J., Zhang, K., Shang, X., Aikawa, M., Zhou, G., Li, J., and Li, H.: Year-round observation of atmospheric inorganic aerosols in urban Beijing: Size distribution, source analysis, and reduction mechanism, Journal of Environmental Sciences, 114, 354-364, https://doi.org/10.1016/j.jes.2021.09.014, 2022b.

Zhao, S., Qi, S., Yu, Y., Kang, S., Dong, L., Chen, J., and Yin, D.: Measurement report: Contrasting

elevation-dependent light absorption by black and brown carbon: lessons from in situ measurements from the highly polluted Sichuan Basin to the pristine Tibetan Plateau, Atmospheric Chemistry and Physics, 22, 14693-14708, 10.5194/acp-22-14693-2022, 2022.

Zhao, Z., Cao, J., Shen, Z., Xu, B., Zhu, C., Chen, L. W. A., Su, X., Liu, S., Han, Y., Wang, G., and Ho, K.: Aerosol particles at a high - altitude site on the Southeast Tibetan Plateau, China: Implications for pollution transport from South Asia, Journal of Geophysical Research: Atmospheres, 118, 10.1002/jgrd.50599, 2013.

Zhu, H., Li, W., Kong, X., and Zhang, X.: Overlooked contribution of salt lake emissions: a case study of dust deposition from the Qinghai-Xizang Plateau, Journal of Geophysical Research: Atmospheres, 130, e2024JD042693, https://doi.org/10.1029/2024JD042693, 2025.